Miner Deposita (2006) 41: 429–452
DOI 10.1007/s00126-006-0069-3

ARTICLE

Lucas J. Marshall · Nicholas H. S. Oliver · Garry J. Davidson

Carbon and oxygen isotope constraints on fluid sources and fluid–wallrock interaction in regional alteration and iron-oxide–copper–gold mineralisation, eastern Mt Isa Block, Australia

Received: 12 November 2004 / Accepted: 1 May 2006 / Published online: 20 June 2006

Abstract The source of metasomatic fluids in iron-oxide–copper–gold districts is contentious with models for magmatic and other fluid sources having been proposed. For this study, $\delta^{18}O$ and $\delta^{13}C$ ratios were measured from carbonate mineral separates in the Proterozoic eastern Mt Isa Block of Northwest Queensland, Australia. Isotopic analyses are supported by petrography, mineral chemistry and cathodoluminescence imagery. Marine meta-carbonate rocks (ca. 20.5‰ $\delta^{18}O$ and 0.5‰ $\delta^{13}C$ calcite) and graphitic meta-sedimentary rocks (ca. 14‰ $\delta^{18}O$ and −18‰ $\delta^{13}C$ calcite) are the main supracrustal reservoirs of carbon and oxygen in the district. The isotopic ratios for calcite from the cores of Na–(Ca) alteration systems strongly cluster around 11‰ $\delta^{18}O$ and −7‰ $\delta^{13}C$, with shifts towards higher $\delta^{18}O$ values and higher and lower $\delta^{13}C$ values, reflecting interaction with different hostrocks. Na–(Ca)-rich assemblages are out of isotopic equilibrium with their metamorphic hostrocks, and isotopic values are consistent with fluids derived from or equilibrated with igneous rocks. However, igneous rocks in the eastern Mt Isa Block contain negligible carbon and are incapable of buffering the $\delta^{13}C$ signatures of CO_2-rich metasomatic fluids associated with Na–(Ca) alteration. In contrast, plutons in the eastern Mt Isa Block have been documented as having exsolved saline CO_2-rich fluids and represent the most probable fluid source for Na–(Ca) alteration. Intrusion-proximal, skarn-like Cu–Au orebodies that lack significant K and Fe enrichment (e.g. Mt Elliott) display isotopic ratios that cluster around values of 11‰ $\delta^{18}O$ and −7‰ $\delta^{13}C$ (calcite), indicating an isotopically similar fluid source as for Na–(Ca) alteration and that significant fluid–wallrock interaction was not required in the genesis of these deposits. In contrast, K- and Fe-rich, intrusion-distal deposits (e.g. Ernest Henry) record significant shifts in $\delta^{18}O$ and $\delta^{13}C$ towards values characteristic of the broader hostrocks to the deposits, reflecting fluid–wallrock equilibration before mineralisation. Low temperature, low salinity, low $\delta^{18}O$ (<10‰ calcite) and CO_2-poor fluids are documented in retrograde metasomatic assemblages, but these fluids are paragenetically late and have not contributed significantly to the mass budgets of Cu–Au mineralisation.

Keywords IOCG · Fluid sources · Australia · Stable isotopes · Carbonate minerals

Editorial handling: B. Gemmell

L. J. Marshall · N. H. S. Oliver
School of Earth Sciences, James Cook University, Townsville, Queensland 4811, Australia

G. J. Davidson
Centre for Ore Deposit Research, University of Tasmania, Private Bag 79, Hobart, Tasmania 7001, Australia

Present address:
L. J. Marshall (✉)
Teck Cominco Limited, #600-200 Burrard Street, Vancouver, British Columbia V6C 3L9, Canada
e-mail: lucas.marshall@teckcominco.com
Tel.: +1-604-8442552

Introduction

The Proterozoic eastern Mt Isa Block of northwest Queensland (Fig. 1) has been at the forefront of research into the role of intrusions in the genesis of iron-oxide–copper–gold mineralisation. Most deposits formed broadly synchronous with emplacement of the Williams and Naraku batholiths (e.g. Ernest Henry and Mt Elliott deposits) and various researchers in the eastern Mt Isa Block have attributed post-peak metamorphic regional alteration and Cu–Au mineralisation to saline fluids derived from predominantly magmatic sources (e.g. de Jong and Williams 1995; Rotherham 1997; Perring et al. 2000; Baker et al. 2001). Variations in fluid chemistry and metasomatic mineral assemblages have been argued to be the result of unmixing of H_2O–CO_2–NaCl fluids (Pollard 2001) as well as progressive fluid–wallrock interaction (Oliver et al. 2004).

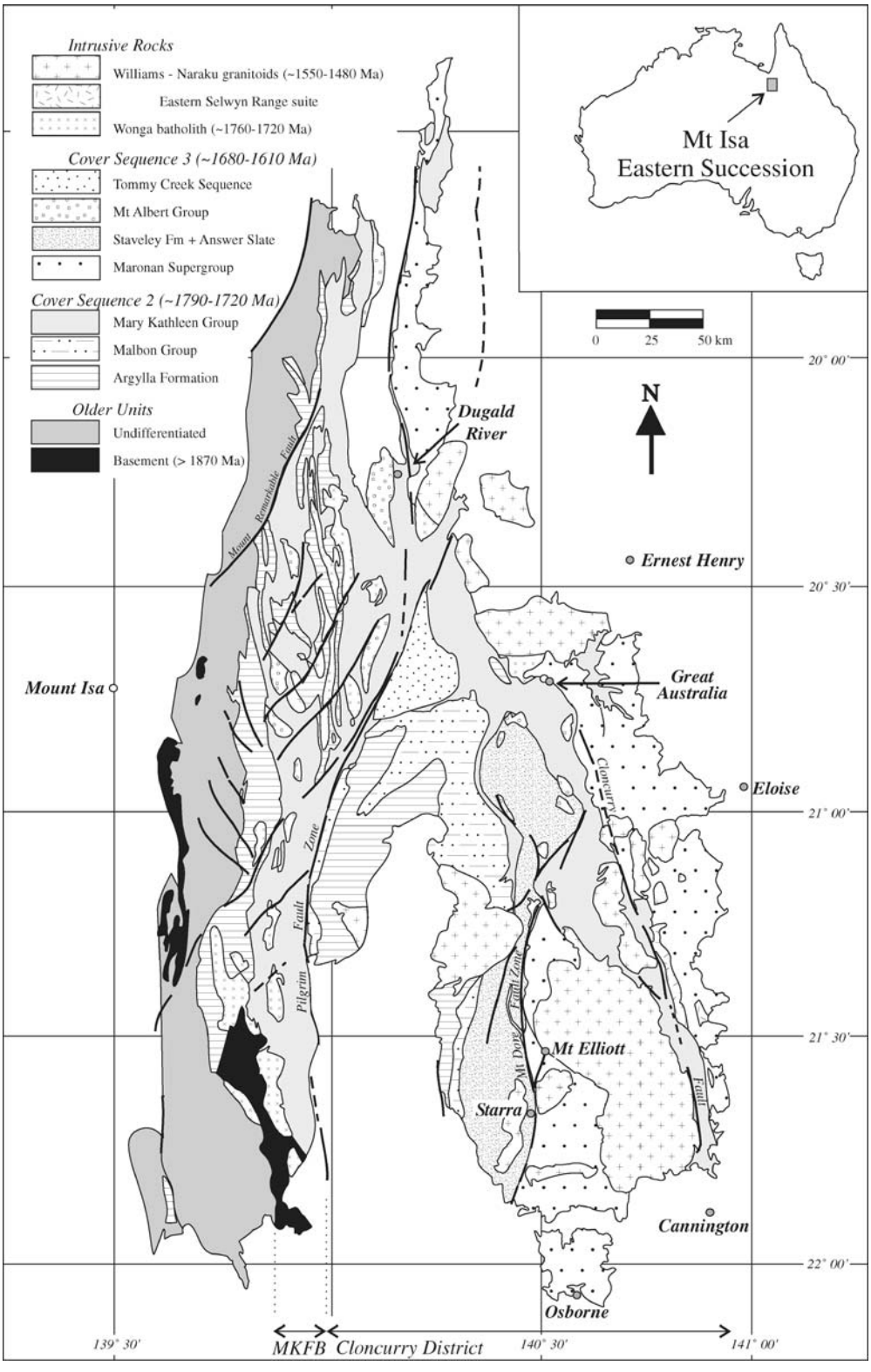

Fig. 1 Simplified geology of the Eastern Succession, Mt Isa Block, modified after Williams (1998)

In other districts, evaporite sequences and playa lakes have been invoked as the principal sources of saline ore fluids, and intrusions are thought to have acted as heat engines driving fluid flow (e.g. Haynes et al. 1995; Barton and Johnson 1996). In still other districts, contemporaneous intrusions have not been recognized and alternate fluid and heat sources seem plausible, although hidden intrusions cannot be ruled out (e.g. Wernecke breccias, Yukon; Thorkelson et al. 2001). Clarifying the role of intrusive bodies in the genesis of iron-oxide–copper–gold

mineralisation is of direct relevance in assessing the prospectivity of newly identified terranes and in establishing terrane-specific exploration criteria.

As pointed out by previous authors (e.g. Farmer and De Paulo 1997; Haynes 2000), where hydrothermal flow paths are long, fluid isotopic signatures may equilibrate with host rock signatures, rendering interpretation of fluid source(s) from isotopic data ambiguous. The generalized isotopic ranges for different rock types and fluid sources also commonly overlap, further complicating the interpretation of fluid sources. This contribution presents a compilation of new and previously published carbon and oxygen isotope data from carbonate minerals in regional host rocks and alteration assemblages and iron-oxide-related Cu–Au mineralisation in the eastern Mt Isa Block. Petrographic observations, cathodoluminescence images and carbonate mineral chemistry support the isotopic data. Examining multiple isotopic systems (i.e. $\delta^{13}C$ and $\delta^{18}O$) from a variety of host rocks and metasomatic assemblages has allowed for the characterization of different isotopic reservoirs that are specific to the eastern Mt Isa Block, removing much of the ambiguity commonly associated with isotopic studies.

Theoretical background, sampling and analytical procedures

Cathodoluminescence and mineral chemistry

Cathodoluminescence (CL) images were acquired by means of digital photography on an ELM-3R luminoscope at the University of Alberta, operating at conditions of ca. 50 mTorr, 10–15 Kv and 0.5–1.0 mA. Chemical analyses were performed along line traverses using a Jeol JXA-840 microprobe at James Cook University, analysing 5-μm spots for 40 s. Element maps were collected using wavelength dispersive spectrometry (WDS).

Carbon and oxygen isotope ratios

Carbon and oxygen stable isotope results from the eastern Mt Isa Block include data from regional host rocks and alteration in the Mary Kathleen Fold Belt and Cloncurry District, as well as data from ore deposits and prospects. All carbon and oxygen isotope ratios are reported relative to V-PDB and V-SMOW, respectively. All analyses were performed on carbonate minerals (calcite and subordinate dolomite and siderite) from both mixed carbonate–silicate ± oxide–sulphide powders and handpicked or micro-drilled pure carbonate samples. The direct comparison of data from calcite, dolomite and siderite is justified as the minerals show small fractionation at high temperatures. At the temperatures of interest (between approximately 300 and 600°C), fractionation between the minerals is not expected to exceed ca. 1‰ for either oxygen or carbon (e.g. Ohmoto and Rye 1979; Golyshev et al. 1981; Zheng 1999). Calcite or dolomite precipitated from an isotopically homogenous H_2O–CO_2–H_2CO_3 fluid at 300°C would record $\delta^{13}C$ and $\delta^{18}O$ values greater by no more than approximately 1 and 4‰, respectively, than if precipitated from the same fluid at 600°C (fractionation factors from O'Neil et al. 1969; Ohmoto and Rye 1979). These values can be taken as an approximation of the maximum temperature effects on fractionation for most data presented in this study. It is notable that the carbonate–CH_4 fractionation has a greater temperature dependence than does fractionation between carbonate and H_2O–CO_2–H_2CO_3 fluids; however, CH_4 is typically absent in fluid inclusions from samples presented in this study (Fu, in preparation). Exceptions exist, however, for the Dugald River, Osborne and Starra deposits where CH_4-bearing fluid inclusions have been documented (e.g. Xu 2000; Davidson and Davis 2001).

Data from regional host rocks and alteration assemblages are summarized in Tables 1 and 2 and are compiled from Oliver et al. (1993; n=84), Hingst (2002; n=6) as well as new data collected for this study (n=106). Analyses were performed on calcite samples at Monash University and the University of Queensland on Finnigan MAT Delta E and MAT 252 mass spectrometers, with CO_2 extracted from calcite by reaction with 100% phosphoric acid at 25°C (McCrae 1950). Precision on in-house standards was 0.1‰.

Data from ore deposits, prospects and their surrounds are compiled from a variety of published sources and unpublished theses (Table 3; n=301) as well as new data collected for this study (Table 4; n=35). The compiled data were analysed at a number of different laboratories, and it was not possible to cross-check results between laboratories. However, all data were collected following the method of McCrae (1950), and reported precision from in-house and international standards is ±0.1 to 0.2‰. Data collected for this study were analysed at Monash University as described above, and at the University of Tasmania, using a Finnigan Isogas 2000 mass spectrometer.

Regional geology

The eastern Mt Isa Block (Fig. 1) refers to the outcropping Eastern Succession of the Mt Isa Inlier and extensions of this terrane covered by younger sedimentary sequences. The region can be divided into two main tectonostratigraphic belts, namely, the Mary Kathleen Fold Belt (MKFB) and Cloncurry District (Fig. 1). Supracrustal rocks in the eastern Mt Isa Block have been assigned by Blake (1987) into Cover Sequences 1, 2 and 3 deposited

Table 1 Regional alteration and host rocks, isotopic data sources

Location	Analyses	Rock types	Source
MKFB	84	Veins, breccias, marbles and calc-silicate rocks	Oliver et al. (1993)
Northern Cloncurry District	6	Marbles and calc-silicate rocks	Hingst (2002)

Table 2 Regional alteration and host rock isotopic data, this study

Sample	Location	Rock types	Mineralogy	$\delta^{18}O$	$\delta^{13}C$
T72b	Tribulation, MKFB	Pegmatite	alb, qtz, cal, act, chl	11.1	−6.6
T72c	Tribulation, MKFB	Calcite pod	cal, act, cpx, qtz, apa, ttn	10.5	−6.3
T72f	Tribulation, MKFB	Calcite pod	cal, act, cpx, qtz, apa, ttn	12.1	−6.0
T72i	Tribulation, MKFB	Calcite pod	cal, act, cpx, qtz, apa, ttn	10.2	−5.8
MP011a	Mt Philp, MKFB	Retrograde breccia	cal, qtz, chl, act, bio, mag, hem, [epi]	12.8	−3.5
MP011d	Mt Philp, MKFB	Retrograde breccia	cal, qtz, chl, act, bio, mag, hem, [epi]	11.0	−4.5
MP011d	Mt Philp, MKFB	Retrograde breccia	cal, qtz, chl, act, bio, mag, hem, [epi]	11.1	−5.1
MP022b	Mt Philp, MKFB	Retrograde breccia	cal, qtz, chl, act, bio, mag, hem, [epi]	11.6	−0.9
MP035	Mt Philp, MKFB	Retrograde breccia	cal, qtz, chl, act, bio, mag, hem, [epi]	11.0	−4.4
BUD42-B1	Budenberri, CD	Na–(Ca) breccia	cal, alb, act, qtz, cpx, scp, ttn, [mag]	12.2	−6.2
BUD67-B1-a	Budenberri, CD	Na–(Ca) breccia	cal, alb, act, cpx, qtz, scp, ttn, [mag]	12.7	−4.6
BUD67-B1-b	Budenberri, CD	Na–(Ca) breccia	cal, alb, act, cpx, qtz, scp, ttn, [mag]	12.4	−4.5
0158-B1	Northern CD	Na–(Ca) breccia	alb, cal, act, opq, [ttn, bio]	10.3	−3.0
0428-B1	Northern CD	Na–(Ca) breccia	alb, act, cal, qtz, mag, [hem, apa, ttn]	11.5	−0.6
1150-B1	Northern CD	Na–(Ca) breccia	alb, cal, act, [ttn, opq]	15.1	−2.8
1374-B1	Northern CD	Na–(Ca) breccia	alb, cal, qtz, act, mag, ttn	9.4	−3.6
1380b-B1	Northern CD	Na–(Ca) breccia	alb, cpx, epi, act, cal, qtz, ttn	11.2	−6.9
1380b-B1	Northern CD	Na–(Ca) breccia	alb, cpx, epi, act, cal, qtz, ttn	11.0	−7.1
0286-B2	Northern CD	Retrograde breccia	hem-fld, cal, qtz, chl, opq	9.8	−1.6
0345-B2	Northern CD	Retrograde breccia	alb, qtz, cal, mag, [chl, pyr]	9.7	−1.2
0606b-B2	Northern CD	Retrograde breccia	qtz, cal, chl, ksp, alb, epi, ttn, opq	7.6	−1.5
1214-B2-a	Northern CD	Retrograde breccia	cal, qtz, hem-fld, hem, chl	7.4	−0.8
1214-B2-b	Northern CD	Retrograde breccia	cal, qtz, hem-fld, hem, chl	4.3	−0.6
1375.05b-B2	Northern CD	Retrograde breccia	alb, cal, qtz, chl, mag, bio, ttn, pyr, hem	11.9	−1.3
1502-B2	Northern CD	Retrograde breccia	cal, qtz, plg, Ksp, chl, opq, [bio, epi, rut, apa, tou]	10.8	−0.7
1845-B2	Northern CD	Retrograde breccia	alb, qtz, cal, mag, [mus, hem]	7.8	−1.8
0029-BT	Northern CD	Transitional breccia	hem-fld, cal, qtz, act, [rie, mag]	11.1	−2.8
1314-BT	Northern CD	Transitional breccia	hem-fld, cal, qtz, bio, act, mag, ttn, hem, chl	9.7	−2.4
1321b-BT	Northern CD	Transitional breccia	hem-fld, cal, qtz, chl, act, bio, mag, hem, [epi]	16.0	−0.3
1351a-BT	Northern CD	Transitional breccia	alb, cal, qtz, act, chl, mag, hem	6.8	−1.8
1375.06c-BT	Northern CD	Transitional breccia	alb, cal, qtz, mag, chl, bio, hem	16.9	−1.1
1561b-BT	Northern CD	Transitional breccia	hem-fld, act, cal, hem, mag, [ttn, chl]	9.1	−2.0
1561b-BT	Northern CD	Transitional breccia	hem-fld, act, cal, hem, mag, [ttn, chl]	11.0	−1.5
0082b-CS-a	Northern CD	Calc-silicate rock	qtz/fld, bio, cal, opq	16.0	−1.7
0082b-CS-b	Northern CD	Calc-silicate rock	qtz/fld, bio, cal, opq	14.4	−0.9
0086-CS	Northern CD	Calc-silicate rock	cal, qtz, fld, chl, bio, [opq, mus]	11.1	−0.5
0135-CS	Northern CD	Calc-silicate rock	qtz/fld, cal, epi	14.0	1.6
0139-CS	Northern CD	Calc-silicate rock	qtz/fld, cal, opq	11.4	−1.3
0158-CS	Northern CD	Calc-silicate rock	qtz/fld, act, cal, [opq]	9.3	−3.0
0325-CS	Northern CD	Calc-silicate rock	cal, qtz, fld, chl, bio, opq	12.6	−0.9
0441-CS	Northern CD	Calc-silicate rock	cal, qtz, fld, bio, [opq, chl]	16.6	2.1
0607-CS	Northern CD	Calc-silicate rock	fld, cal, qtz, opq	9.6	0.7
0804-CS	Northern CD	Calc-silicate rock	qtz, bio, cal, fld, mus, chl	10.2	−0.4
0865-CS	Northern CD	Calc-silicate rock	qtz, fld, cal, bio, [opq]	13.4	1.8
1375.05b-CS-a	Northern CD	Calc-silicate rock	fld, qtz, cal, bio, hem	11.9	−1.4
1375.05b-CS-b	Northern CD	Calc-silicate rock	fld, qtz, cal, bio, hem	11.9	−1.6
1375.09-CS	Northern CD	Calc-silicate rock	cal, qtz, fld, bio, opq	12.5	0.3
1375.09-CS	Northern CD	Calc-silicate rock	cal, qtz, fld, bio, opq	12.4	0.4
1375.10-CS	Northern CD	Calc-silicate rock	cal, qtz, bio, ksp, scp, opq	17.5	0.8
1384a-CS	Northern CD	Calc-silicate rock	qtz, alb, cal, act, bio, opq	13.6	−3.1
1426-CS	Northern CD	Calc-silicate rock	fld, cal, qtz, opq	12.8	−0.8

Table 2 (continued)

Sample	Location	Rock types	Mineralogy	$\delta^{18}O$	$\delta^{13}C$
1502-CS	Northern CD	Calc-silicate rock	fld, cal, qtz, opq	10.1	−1.1
0036-M-a	Northern CD	Marble	cal, qtz, bio	16.3	1.8
0036-M-b	Northern CD	Marble	cal, qtz	10.4	0.5
0038-M-a	Northern CD	Marble	cal, qtz, bio, [mus, opq]	20.1	2.1
0038-M-b	Northern CD	Marble	cal, qtz	14.3	1.8
0135-M-a	Northern CD	Marble	cal, qtz, bio, [chl]	14.3	2.4
0135-M-b	Northern CD	Marble	cal, chl	20.2	2.3
0140-M	Northern CD	Marble	qtz, cal	7.6	−0.7
0282-M-a	Northern CD	Marble	cal, qtz, bio, [chl, opq]	12.1	0.1
0282-M-b	Northern CD	Marble	cal, qtz, bio	8.9	−1.4
0352-M	Northern CD	Marble	cal, qtz, hem, [chl]	11.8	1.2
0433-M-a	Northern CD	Marble	cal, qtz, act	12.2	1.6
0433-M-b	Northern CD	Marble	cal	10.2	0.5
0494-M-a	Northern CD	Marble	cal, bio, qtz, chl, [tou, fld, opq]	9.7	−0.7
0494M-b	Northern CD	Marble	cal, bio, qtz, chl, [tou, fld, opq]	9.6	−0.7
0494-M-c	Northern CD	Marble	cal, bio, qtz, chl	10.8	−0.9
0607-M-a	Northern CD	Marble	cal, qtz, chl, [plg, opq]	14.7	1.7
0607-M-b	Northern CD	Marble	cal, qtz, chl, [plg, opq]	14.7	1.8
0607-M-c	Northern CD	Marble	cal, qtz, chl, [plg, opq]	12.8	1.5
0865-M	Northern CD	Marble	cal, qtz, bio	15.2	1.5
1047Ma	Northern CD	Marble	cal, qtz, act, bio, opq	17.4	1.8
1047Mb	Northern CD	Marble	cal, [qtz, bio]	18.5	1.9
1375.09Ma	Northern CD	Marble	cal, qtz, bio, [ttn]	16.6	1.2
1375.09Mb	Northern CD	Marble	cal, qtz, bio, [ttn]	13.5	0.9
1441bMa	Northern CD	Marble	cal, qtz, alb, ksp, tou	12.5	0.7
1441bM-b	Northern CD	Marble	cal, qtz, alb, ksp, tou	11.4	0.0
1450a-M	Northern CD	Marble	cal, qtz, plg, opq	14.5	1.7
0432-SC	Northern CD	Soldiers Cap	qtz, cal, [chl, opq]	11.2	−2.2
1207-SC	Northern CD	Soldiers Cap	cal, qtz, gra	14.0	−4.9
1260SC	Northern CD	soldiers Cap	cal, alb, qtz, mag, hem	16.2	−7.3
1263-SC	Northern CD	Soldiers Cap	cal, act, gra	8.9	−7.8
1264-SC	Northern CD	Soldiers Cap	cal, alb, act, qtz, mag, [bio]	14.2	−7.5
1266b-SC	Northern CD	Soldiers Cap	cal, alb	11.1	−13.1
1266b-SC	Northern CD	Soldiers Cap	cal, alb	11.1	−13.2
0202-V1	Northern CD	Na–(Ca) vein	cal, act, qtz, mag	13.5	−1.7
1375.04-V1	Northern CD	Na–(Ca) vein	cal, qtz, bio, act, mag	17.6	−1.1
1384a-V1	Northern CD	Na–(Ca) vein	cal, act, alb, opq, qtz, ttn	13.7	−3.1
1384g-V1	Northern CD	Na–(Ca) vein	cal, qtz, alb, act, chl	14.0	−3.3
1686-V1	Northern CD	Na–(Ca) vein	cal, mag, qtz	11.4	−5.6
1714-V1	Northern CD	Na–(Ca) vein	cal, qtz, act, bio, cpy, pyr, mag	11.7	−6.9
0286-V2	Northern CD	Retrograde vein	cal, [qtz, opq]	8.5	−1.5
1375.06d-V2	Northern CD	Retrograde vein	qtz, pyr, cal, hem, mag, cpy	11.9	−1.4
1506-V2	Northern CD	Retrograde vein	cal, qtz, plg, ksp, hem	11.0	−1.2
0082b-V3-b	Northern CD	Rock-buffered vein	cal, bio, qtz, opq	17.7	−1.3
0082b-V3-a	Northern CD	Rock-buffered vein	cal, bio, qtz, opq	14.4	−1.1
0086-V3	Northern CD	Rock-buffered vein	cal, qtz, bio, [opq]	15.7	−0.7
0325-V3	Northern CD	Rock-buffered vein	cal, qtz, [bio, opq, chl]	14.5	−0.4
0441-V3	Northern CD	Rock-buffered vein	cal, qtz	18.1	2.1
0804-V3	Northern CD	Rock-buffered vein	cal, qtz, opq	15.8	−0.1
0865-V3	Northern CD	Rock-buffered vein	cal, qtz, bio	16.2	1.8
1375.09-V3	Northern CD	Rock-buffered vein	cal, qtz	10.4	0.2

Table 2 (continued)

Sample	Location	Rock types	Mineralogy	$\delta^{18}O$	$\delta^{13}C$
1394-V3	Northern CD	Rock-buffered vein	cal, bio, qtz	13.6	0.1
1426-V3	Northern CD	Rock-buffered vein	cal, qtz	10.6	−1.3
1448-V3	Northern CD	Rock-buffered vein	cal, qtz, ksp, alb, chl, cpy, mag, hem, pyr, [bio]	12.9	0.2
0029-VT	Northern CD	Transitional vein	cal, qtz, [hem-fld, cal, qtz, act, rie, mag]	9.1	−3.7

Oxygen and carbon isotope values reported relative to V-SMOW and PDB, respectively
MKFB Mary Kathleen Fold Belt, *CD* Cloncurry District, *act* actinolite, *alb* albite, *apa* apatite, *bio* biotite, *cal* calcite, *chl* chlorite, *cpx* clinopyroxene, *cpy* chalcopyrite, *epi* epidote, *fld* feldspar, *gra* graphite, *hem* hematite, *hem-fld* hematite-stained feldspar, *ksp* K-feldspar, *mag* magnetite, *mus* muscovite, *opq* unidentified opaque, *plg* plagioclase, *pyr* pyrite, *qtz* quartz, *rie* riebeckite, *rut* rutile, *scp* scapolite, *tou* tourmaline, *ttn* titanite

Table 3 Ore deposits, isotopic data sources

Location	Analyses	Commodity	Cover Sequence	Host lithology	Source(s)
Mt Freda style	45	Au–Cu	3	TCV/MNQ	Davidson and Garner (1997)
Great Australia	12	Cu–Au–Co	2/3	TCV/CF	Davidson and Garner (1997), Cannell and Davidson (1998)
Fairstar	3	Cu–Au	3	TCV	Davidson and Garner (1997)
Monakoff	18	Cu–Au	3	TCV/MNQ	Davidson and Garner (1997)
Mt Dore	11	Cu	3	KF	Beardsmore (1992)
Starra	81	Au–Cu	3	SF	Davidson (1989), Rotherham et al. (1998)
Greenmount	15	Cu–Au	3	MS	Krcmarov (1995)
Dugald River	42	Zn–Pb–Ag	3	LCD	Porter (1990), Dixon and Davidson (1996)
Plume	6	Cu–Au	3	KF or SF	Fletcher (1999)
Houdini	4	Cu	3	SF/LCF or MNQ	Weston (2000)
Ernest Henry	59	Cu–Au	2	MFC/MMB	Twyerould (1997), Mark et al. (1999)
Osborne	5	Cu–Au	3	SF	Davidson (1989)

MNQ Mt Norna Quartzite, *KF* Kuridala Formation, *MFC* Mt Fort Constantine volcanics, *MS* undifferentiated Maronan Supergroup, *MMB* marble matrix breccia

during distinct rift events at ca. 1870–1840, 1790–1720 and 1680–1620 Ma, respectively. Calc-silicate rocks, marbles, meta-siltstones, and mafic and felsic meta-volcanic rocks of the Mary Kathleen Group (Cover Sequence 2), including the Corella Formation, dominate the Mary Kathleen Fold Belt and much of the Cloncurry District. This sequence contains abundant metamorphic scapolite and is likely the metamorphosed equivalent of evaporitic marine carbonates (e.g. Oliver et al. 1992).

Cover Sequence 3 stratigraphy, including the Soldiers Cap Group, was emplaced over Cover Sequence 2, probably by thrusting, in an early structural event (D_1). Upright, north-trending folds and pervasive fabric development are most commonly attributed to D_2 (e.g. O'Dea et al. 1997) and formed broadly synchronous with upper greenschist to amphibolite facies peak metamorphism at ca. 1600–1575 Ma (Page and Sun 1998; Giles and Nutman 2002; Hand and Rubatto 2002).

Emplacement of the Williams and Naraku batholiths (ca. 1550–1500 Ma) overlapped in time with retrograde deformation (D_3) and with extensive metasomatic fluid flow that is the focus of this contribution. Spherulites and unidirectional solidification textures documented in the Mt Angelay igneous complex and at the Lightning Creek prospect have been interpreted to record release of a fluid phase during igneous crystallization, and these and similar intrusive bodies have been invoked as likely sources for fluids responsible for regional Na–(Ca) alteration (Mark and Foster 2000; Perring et al. 2000).

Numerous examples of iron-oxide-related Cu ± Au mineralisation exist throughout the Cloncurry District and to a lesser extent the MKFB and include such deposits as Ernest Henry, Osborne, Starra and Mt Elliott (Fig. 1). With the exception of Osborne, these deposits formed broadly synchronous with emplacement of the Williams and Naraku batholiths (e.g. Oliver et al. 2004). Despite similarities in relative timing, the deposits exhibit significant variations in mineralogy. For example, Mt Elliott, which lies adjacent to the Squirrel Hills pluton, exhibits a skarn-like albite-, diopside-, scapolite-, actinolite-, calcite-, magnetite- and sulphide-rich mineral assemblage (Little 1997; Wang and Williams 2001). In contrast, Ernest Henry is distal to any known synchronous intrusions and is characterized by a K-feldspar-, biotite-, amphibole-, magnetite-, calcite- and sulphide-rich mineral assemblage (Mark and Crookes 1999).

Isotopic sample suites

The mineralogy, occurrence and characteristic textures of isotopic sample suites presented in this contribution are

Table 4 Ore deposits isotopic data, this study

Location	Sample	Commodity	Cover Sequence	Host lithology	Syn-Cu–Au	Description	$\delta^{18}O$	$\delta^{13}C$
Ernest Henry	EH.01a	Cu–Au	2	MMB	No	MMB	15.7	−2.2
Ernest Henry	EH.01b	Cu–Au	2	MFC	Yes	milled ore breccia	15.6	−2.1
Ernest Henry	EH.02a	Cu–Au	2	MMB	No	MMB	15.0	−1.6
Ernest Henry	EH.02b	Cu–Au	2	MMB	No	MMB	15.2	−1.7
Ernest Henry	EH.02b	Cu—Au	2	MMB	No	MMB	15.2	−1.7
Ernest Henry	EH.02c	Cu–Au	2	MFC	Yes	Milled ore breccia	15.2	−1.4
Ernest Henry	EH.03	Cu–Au	2	MFC	No	Na–Ca infill	12.4	−4.0
Ernest Henry	EH.04a	Cu–Au	2	MMB	No	MMB	15.6	−1.8
Ernest Henry	EH.04a	Cu–Au	2	MMB	No	MMB	15.8	−1.6
Ernest Henry	EH.04b	Cu–Au	2	MFC	Yes	Milled ore breccia	14.9	−1.8
Ernest Henry	EH.04c	Cu–Au	2	MFC	Yes	Milled ore breccia	14.6	−1.4
Ernest Henry	EH.05a	Cu–Au	2	MFC	Yes	Milled ore breccia	11.4	−1.5
Ernest Henry	EH.05b	Cu–Au	2	MFC	Yes	Milled re breccia	11.4	−1.7
Ernest Henry	EH.06	Cu–Au	2	MFC	Yes	Milled ore breccia	14.0	−1.0
Ernest Henry	EH.07	Cu–Au	2	MFC	No	Na–Ca infill	12.6	−4.5
Ernest Henry	EH.08	Cu–Au	2	MFC	No	Na–Ca infill	11.3	−3.6
Ernest Henry	EH.09	Cu–Au	2	MFC	Yes	Milled ore breccia	8.3	−3.5
Ernest Henry	EH.10	Cu–Au	2	MMB	No	MMB	14.2	−2.7
Ernest Henry	EH.10	Cu–Au	2	MMB	No	MMB	14.0	−2.4
Eloise	EL.01	Cu–Au	3	MNQ	Yes	Mineralised vein	8.9	−8.6
Eloise	EL.02	Cu–Au	3	MNQ	Yes	Mineralised vein	10.0	−8.9
Eloise	EL.03	Cu–Au	3	MNQ	Yes	Mineralised vein	10.0	−9.3
Eloise	EL.04	Cu–Au	3	MNQ	Yes	Mineralised vein	9.9	−9.8
Eloise	EL.04	Cu–Au	3	MNQ	Yes	Mineralised vein	9.9	−9.8
Mt Elliott	ME.01	Cu–Au	3	KF	Yes	Ore breccia infill	11.7	−9.0
Mt Elliott	ME.01	Cu–Au	3	KF	Yes	Ore breccia infill	12.1	−9.2
Mt Elliott	ME.02	Cu–Au	3	KF	Yes	Ore breccia infill	13.0	−8.9
Mt Elliott	ME.03	Cu–Au	3	KF	Yes	Ore breccia infill	11.3	−6.4
Mt Elliott	ME.03	Cu–Au	3	KF	Yes	Ore breccia infill	11.0	−6.7
Mt Elliott	ME.04	Cu–Au	3	KF	Yes	Ore breccia infill	11.8	−9.4
Starra	D8-3/9858	Au–Cu	3	SF	Yes	Ironstone hosted	25.7	−16.9
Starra	D9-5A/9876	Au–Cu	3	SF	Yes	Ironstone hosted	22.8	−16.6
Starra	St115 2/9860	Au–Cu	3	SF	Yes	Ironstone hosted	25.9	−14.3
Osborne	TT132B/9861	Cu–Au	3	MS	Yes	Ironstone hosted	24.0	−7.1
Osborne	TT66/9862	Cu–Au	3	MS	Yes	Wallrock-hosted vein	18.8	−3.6

Oxygen and carbon isotope values reported relative to V-SMOW and PDB respectively
MNQ Mt Norna Quartzite, *KF* Kuridala Formation, *MFC* Mt Fort Constantine volcanics, *MS* undifferentiated Maronan Supergroup, *MMB* marble matrix breccia

described below. Photographs of representative samples are presented in Fig. 2. Photomicrographs of carbonate mineral textures commonly observed using cathodoluminescence are presented in Fig. 3 and ternary diagrams of carbonate composition are given in Fig. 4.

Marbles, calc-silicate rocks and meta-siltstones

Much of the eastern Mt Isa Block is underlain by the meta-evaporitic Corella Formation. Carbonate-bearing lithologies include marbles (>50% carbonate), calc-silicate rocks (10–50% carbonate) and meta-siltstones (<10% carbonate) with variable components of metamorphic biotite, quartz, K-feldspar, titanite, magnetite and scapolite. In the Mary Kathleen Fold Belt, where amphibolite facies conditions predominate, metamorphic amphiboles, clinopyroxene and garnet are also common. Altered samples contain variable proportions of actinolite, albite, magnetite, hematite, chlorite, muscovite and tourmaline. Calcite grains range from predominantly clean, polygonal calcite grains with smoothly curved boundaries to irregular-shaped grains with very abundant twins (commonly curved) and irregular and mottled grain boundaries. Given the common tectonothermal history of the samples and the fact that calcite readily recrystallizes at moderate to high temperatures, irregular calcite grain boundaries were likely produced at relatively low temperatures, late in the tectonothermal history of the terrane.

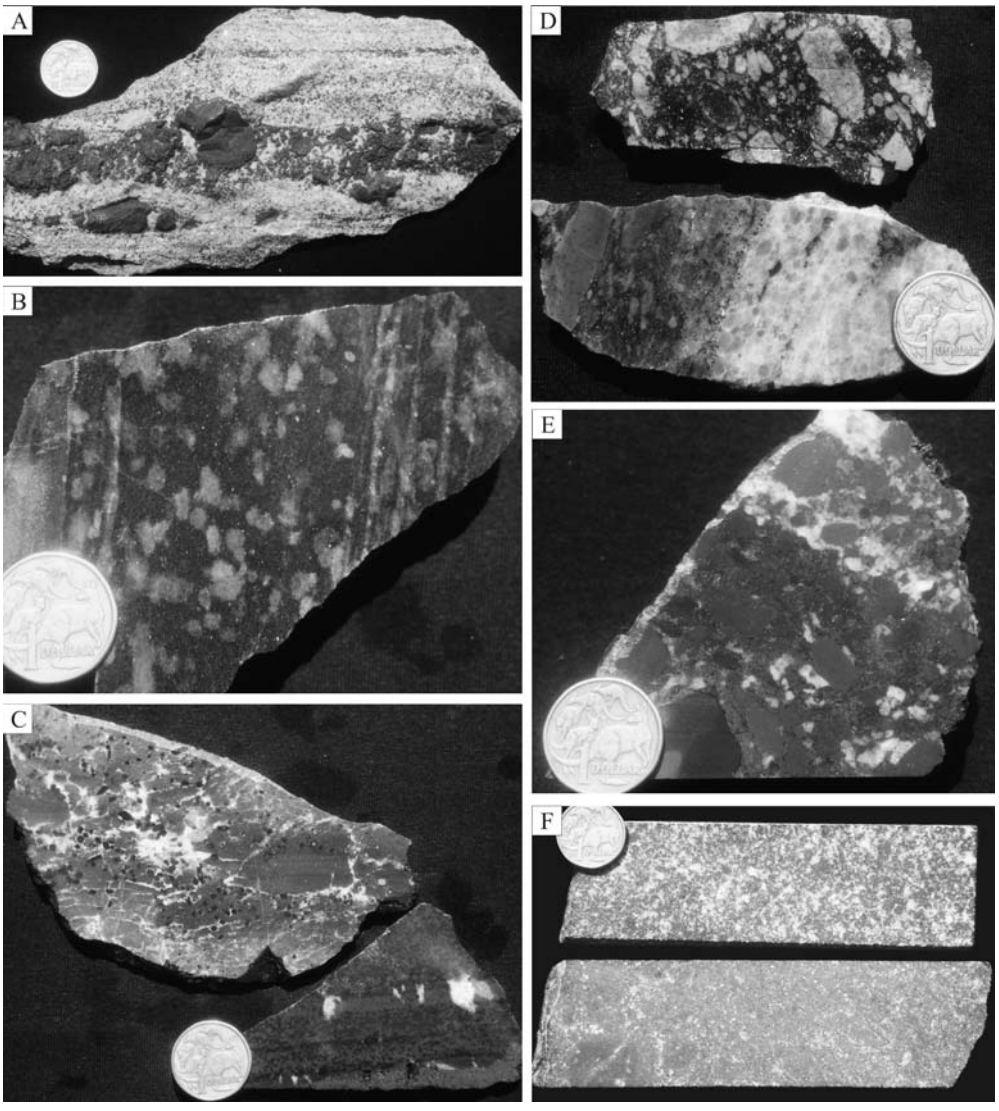

Fig. 2 Photographs of representative samples analysed for this study. The diameter of the coin in each photo is 2.4 cm. **a** Corella Formation marble, with fractured and boudinaged meta-siltstone layer. **b** Unaltered, calcite–biotite–K-feldspar–scapolite-rich calc-silicate rock. **c** Scapolitic calc-silicate rocks with "rock-buffered" calcite veins, lacking visible alteration. **d** Na–(Ca) altered breccias, with albite- and actinolite-rich matrix and albitised clasts. The lower sample is cut by a calcite-rich vein. **e** Retrograde, chlorite-bearing breccia with a large component of calcite infill (*white*). (**f**) Infill- and matrix-supported Ernest Henry ore breccia

Cloncurry District marbles investigated by CL imagery preserve dull orange-luminescing cores to calcite grains, commonly with an interconnected network of bright orange- to yellow-luminescing grain boundaries, twins and microfractures. Figure 5 presents two CL images and associated microprobe traverses from Cloncurry District marble samples. Bright-luminescing calcite is visible along grain boundaries and twins and completely replaces some grains. Microprobe analyses indicate that dull-luminescing calcite grain cores are characterized by very homogenous concentrations of MgO and FeO (total FeO ± Fe_2O_3 analysed as FeO). Areas of bright-luminescing calcite have slightly depleted background concentrations of MgO and FeO relative to dull-luminescing calcite and include intermittent spikes in FeO ± MgO concentrations. These spikes are inferred to record small inclusions of hematite and chlorite, giving the bright-luminescing calcite a mottled appearance. Coarser-grained hematite and chlorite have been identified in these samples petrographically. The chemical variations corresponding with the CL images are also evident in wavelength dispersive microprobe element maps (Fig. 5) and confirm that, in areas of bright-luminescing calcite, MgO and FeO are stripped from calcite and concentrated into small mineral inclusions.

Rock-buffered veins

Within Corella Formation stratigraphy, veins characterised by calcite ± quartz and biotite infill assemblages that lack mesoscopic evidence for associated wallrock alteration have been termed rock-buffered veins in this study. It is noted, however, that such veins may record varying degrees of chemical and/or isotopic disequilibrium with their immediate host rocks. While the veins cannot be attributed to a distinct metasomatic event, they cut peak metamorphic fabrics and mineral assemblages.

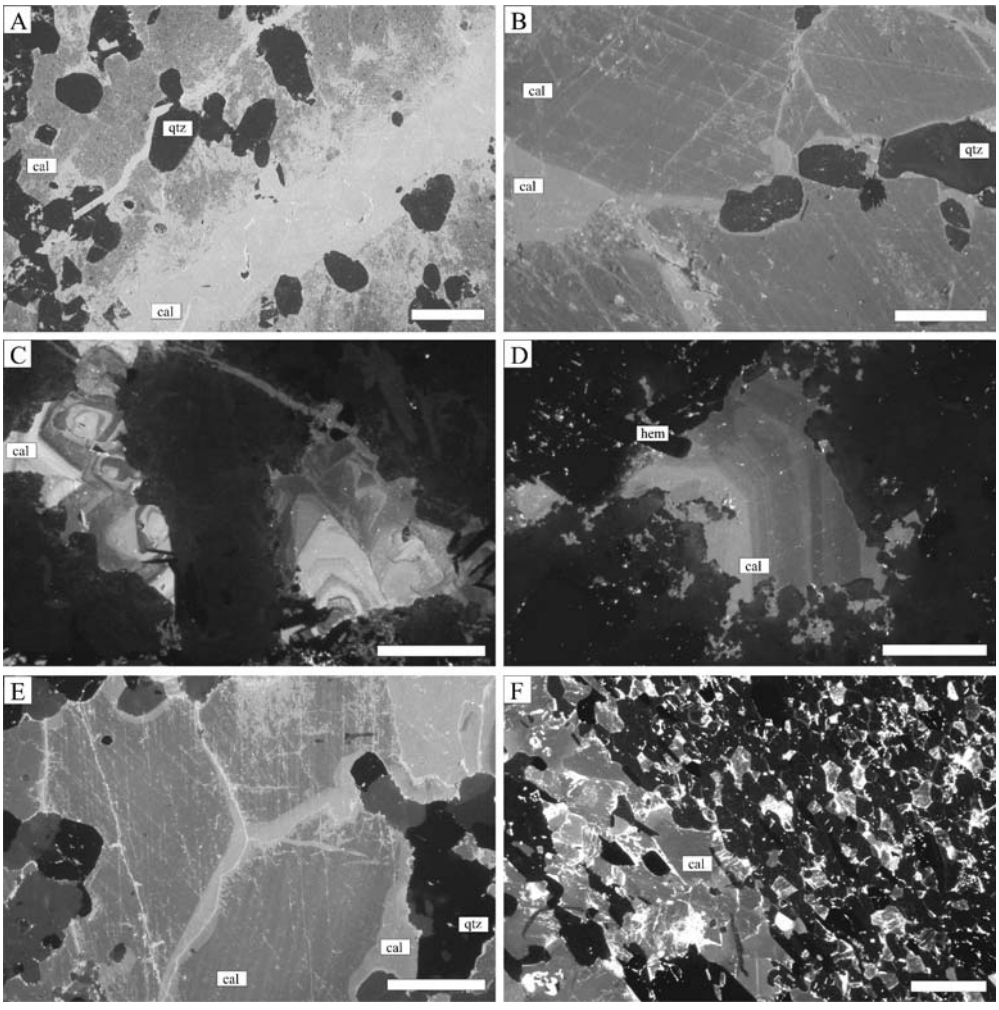

Fig. 3 CL images of textures commonly observed in eastern Mt Isa Block calcite grains. All *scale bars* are 500 μm. **a** Bright-luminescing calcite-microfractures in Cloncurry District marble are not visible in transmitted light but common in CL images. **b** Predominantly homogenous medium- to bright-luminescing infill calcite associated with albite–actinolite-rich alteration shows some grain boundary replacement by brighter-luminescing calcite. **c**, **d** Infill in retrograde breccias and veins commonly preserves growth banding and, in all cases, lacks grain boundary alteration. **e** Bright-luminescing calcite grain boundary alteration in the Ernest Henry ore breccia and **f** the Ernest Henry marble matrix breccia

Carbonaceous meta-sedimentary rocks

Carbonaceous meta-sedimentary rocks are relatively abundant within Cover Sequence 3 of the Cloncurry District. Carbonaceous sequences include calcite–actinolite–graphite-rich calc-silicate rocks within the Soldiers Cap Group and the carbonaceous and calcareous Dugald Slates of the Lady Clayre Dolomite (Mount Albert Group) host to the stratabound Dugald River Zn–Pb–Ag deposit (38 Mt at 13.0% Zn, 2.1% Pb and 42 g/t Ag; Newberry et al. 1993).

Sodic–(calcic) alteration systems: ca. 1555–1520 Ma

Breccias and veins associated with sodic–(calcic) alteration are characterized by albite, actinolite and calcite ± clinopyroxene, magnetite, quartz, scapolite, biotite, titanite and apatite mineral assemblages. Calcite occurs as infill in veins and breccias and as altered breccia matrix. Veining, brecciation and alteration were focussed in part at contacts between units marked by significant competence contrasts and within brittle–ductile shear zones. Albite- and actinolite-rich alteration assemblages replace peak metamorphic mineral assemblages and were formed predominantly at ca. 1555–1520 Ma (Oliver et al. 2004). CL images from calcite breccia and vein infill associated with sodic–(calcic) alteration assemblages typically reveal homogenous, moderate- to bright-luminescing calcite (Fig. 6a). Growth zoning is weakly developed or more commonly absent. In some cases, infill calcite exhibits replacement by brighter-luminescing calcite along grain boundaries and microfractures (Fig. 3b), with textures similar to those described above for marbles. Networks of brighter-luminescing calcite were not chemically distinguishable from the main episode of calcite infill. Microprobe traverses indicate that infill calcite associated with sodic–(calcic) alteration is chemically homogenous, with very low concentrations of FeO, MgO and MnO (Fig. 6a).

Transitional and retrograde breccias and veins: <1525 Ma (?)

Transitional breccias and veins are marked by similar mineralogy to sodic–(calcic) breccias and veins, but with the presence of significant chlorite ± K-feldspar, hematite and hematite-dusting of feldspars. In some samples, the lower-temperature chloritic assemblages clearly replace higher-temperature actinolitic assemblages, while in other samples chlorite and actinolite appear to be coeval.

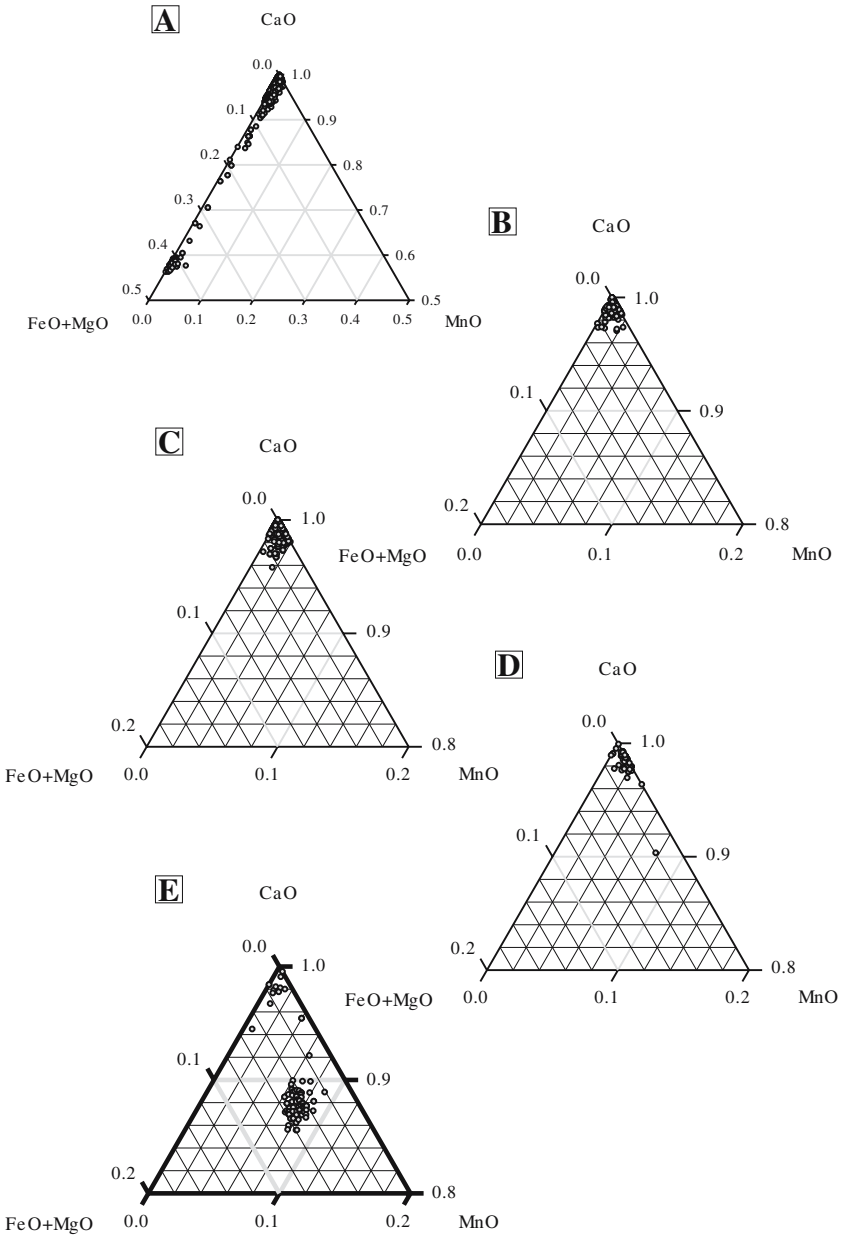

Fig. 4 Ternary diagrams illustrating the chemical range for carbonates in **a** Cloncurry District marbles, **b** sodic–(calcic) breccias and veins, **c** retrograde breccias and veins, **d** Ernest Henry ore breccia and **e** the Ernest Henry marble matrix breccia

Retrograde breccias and veins are characterized by calcite and chlorite ± quartz, hematite, K-feldspar, epidote and biotite mineral assemblages and lack actinolite or significant albite alteration. Calcite occurs as both infill and alteration of breccia matrix. The breccias and veins are commonly located within dilational fault zones and are marked by bright-red coloration due to associated hematite dusting and/or K-feldspar alteration. The timing of these breccias is constrained to be younger than the high-temperature alteration by the paragenetic overprinting of high-temperature alteration.

Calcite infill associated with retrograde breccias and veins commonly shows complex growth zoning in CL images, marked by alternating moderate- and bright-luminescing calcite (Figs. 3c,d and 6b). All infill record very low concentrations of FeO, MgO and MnO (Fig. 6b) and chemical analyses were on the whole indistinguishable from calcite infill associated with sodic–(calcic) assemblages (Fig. 4). Calcite in retrograde breccias and veins lacks the networks of bright-luminescing grain boundary calcite evident in marbles and sodic–(calcic) assemblages.

Cu–Au mineralisation

Ernest Henry deposit

The Ernest Henry deposit (166 Mt at 1.1% Cu and 0.55 g/t Au; Ryan 1998) is the largest Cu–Au occurrence in the eastern Mt Isa Block. Variably sheared and brecciated Mt Fort Constantine (MFC) felsic volcanic rocks and subordinate calc-silicate rocks of the uppermost

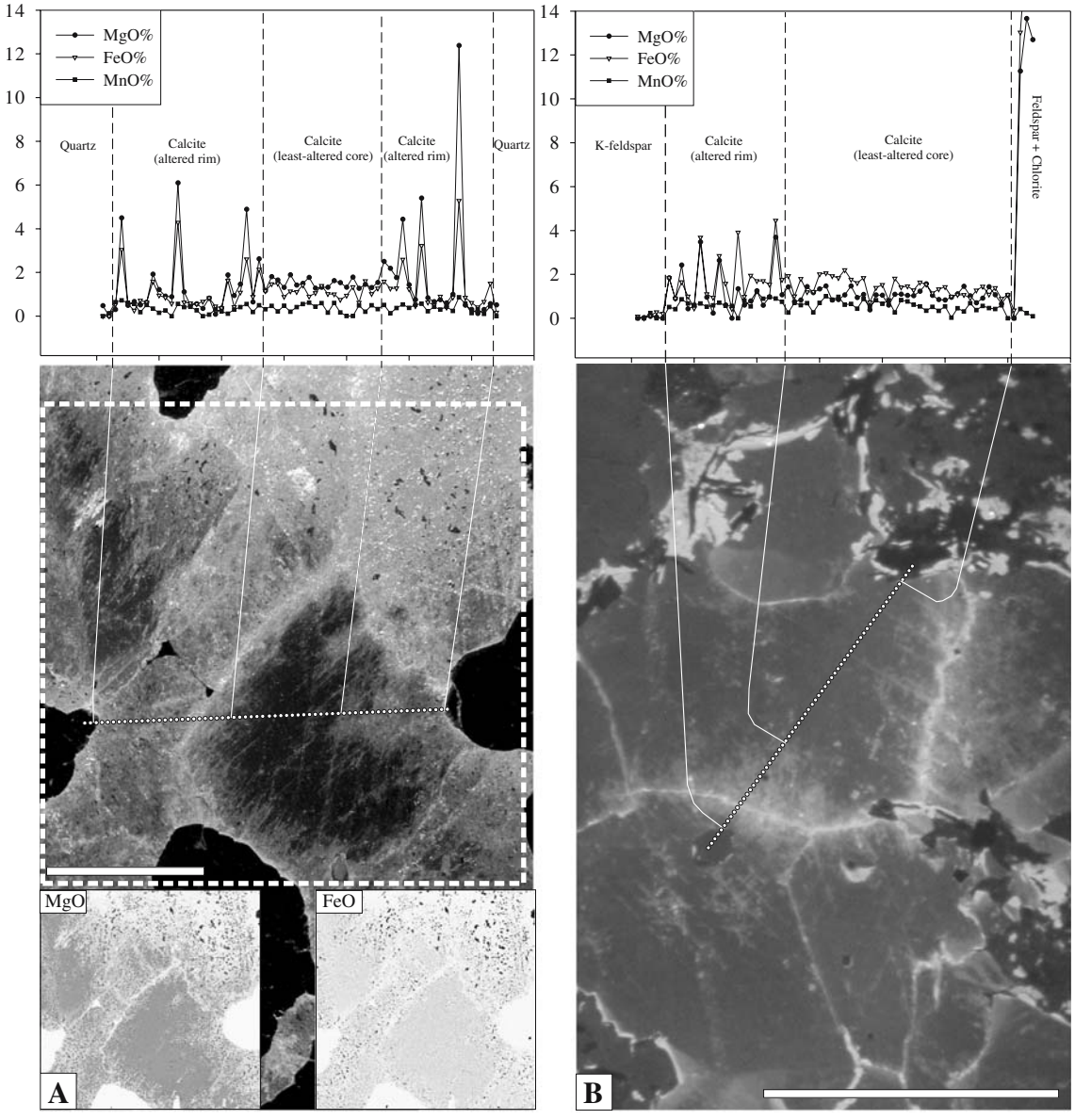

Fig. 5 CL images and associated microprobe traverse from Cloncurry District marbles. The bright-luminescing calcite networks are marked by a redistribution of FeO and MgO from metamorphic calcite into fine-grained inclusions of chlorite and hematite (total Fe reported as FeO). *Dashed square* indicates the position of MgO and FeO WDS element maps (*inset*). The *dark areas* in element maps are enriched in MgO or FeO. *Scale bars*=500 μm

Mary Kathleen Group (Cover Sequence 2) dominate hanging-wall stratigraphy at the deposit. Economic Cu–Au mineralisation is hosted by matrix- to infill-supported milled breccias. Breccia clasts are derived from the host volcanic rocks and are predominantly rounded. Ore mineralogy is dominated by K-feldspar, magnetite, carbonate, quartz, biotite, pyrite and chalcopyrite and occurs as both infill in the ore breccia and as alteration of breccia clasts and matrix.

A cathodoluminescence investigation of the Ernest Henry ore breccia reveals moderate- to bright-luminescing calcite and a lack of growth banding (Fig. 7a). Some samples preserve significant replacement of coarse-grained calcite by brighter-luminescing calcite along grain boundaries and twins (Fig. 3e). Ore breccia calcite contains low concentrations of FeO, MgO and MnO, but with higher ratios of MnO to FeO + MgO than for other infill assemblages in the district (Fig. 4). It is notable that anomalous MnO concentrations are recorded immediately adjacent to some magnetite grains (Fig. 7a), and Ernest Henry magnetite has been shown to contain very high concentrations of Mn (Marshall 2003). As such, the enrichment in calcite MnO content adjacent to magnetite grains may reflect diffusional processes.

The footwall to the Ernest Henry deposit is dominated by a calcite-rich, intensely sheared unit termed “marble matrix breccia” (MMB) by mine geologists. The MMB is a medium-grained (most grains <5 mm), calcite–actinolite–biotite–apatite-rich rock that commonly contains >10% disseminated Mn-rich magnetite (Marshall 2003). Mark et

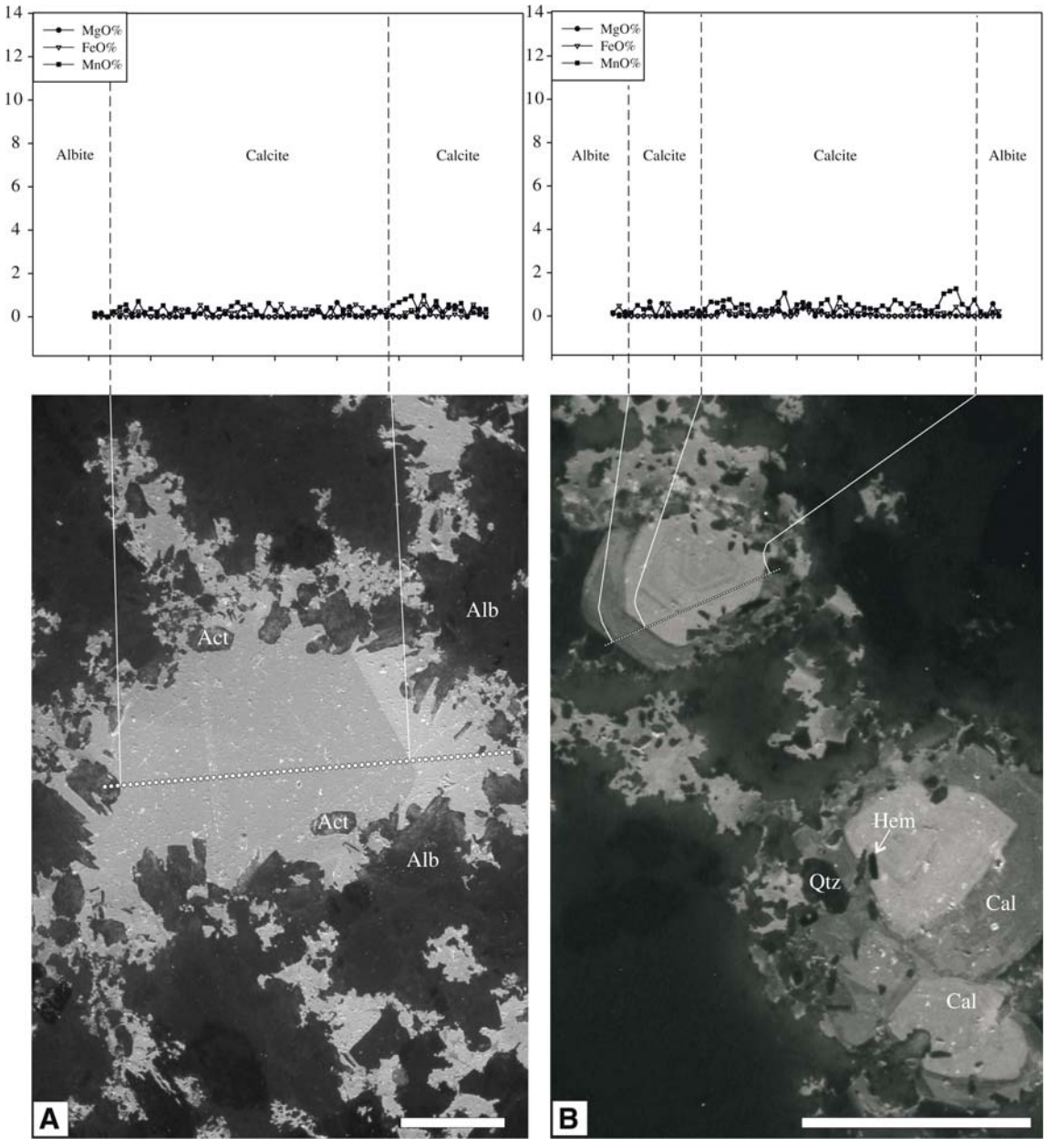

Fig. 6 CL images and microprobe traverses for calcite infill in both **a** sodic–(calcic) breccias and **b** retrograde breccias reveal chemically homogenous calcite with low concentrations of FeO, MgO and MnO. Growth bands do not record measurable chemical variations. *Scale bars*=500 μm

al. (1999) interpreted the MMB as consisting predominantly of hydrothermal infill. In contrast, Marshall (2003) argued, based on textural similarities with Cloncurry District marbles, that the MMB is indeed a marble, albeit intensely sheared and metasomatised.

MMB calcite has a predominantly homogeneous, moderate-luminescing CL response, although bright-luminescing calcite is locally noted along some grain boundaries and replacing some actinolite grains (Fig. 7b). Some MMB calcite is chemically similar to Corella Formation marble calcite, but most MMB calcite contains significantly elevated MnO concentrations (Fig. 4).

Great Australia deposit

Great Australia is a small Cu–Au–Co deposit hosted by Toole Creek Volcanics (TCV) of the Soldiers Cap Group (Cover Sequence 3), adjacent to and within a splay of the Cloncurry fault that marks a sheared contact with Corella Formation marbles and calc-silicate rocks (Cover Sequence 2) to the west (Fig. 1). The deposit contains a supergene resource of 1.7 Mt at 1.2% Cu, with a larger undefined hypogene orebody (Cannell and Davidson 1998). Hypogene mineralisation is characterized by carbonate–(calcite and dolomite) and actinolite-rich lodes with variable

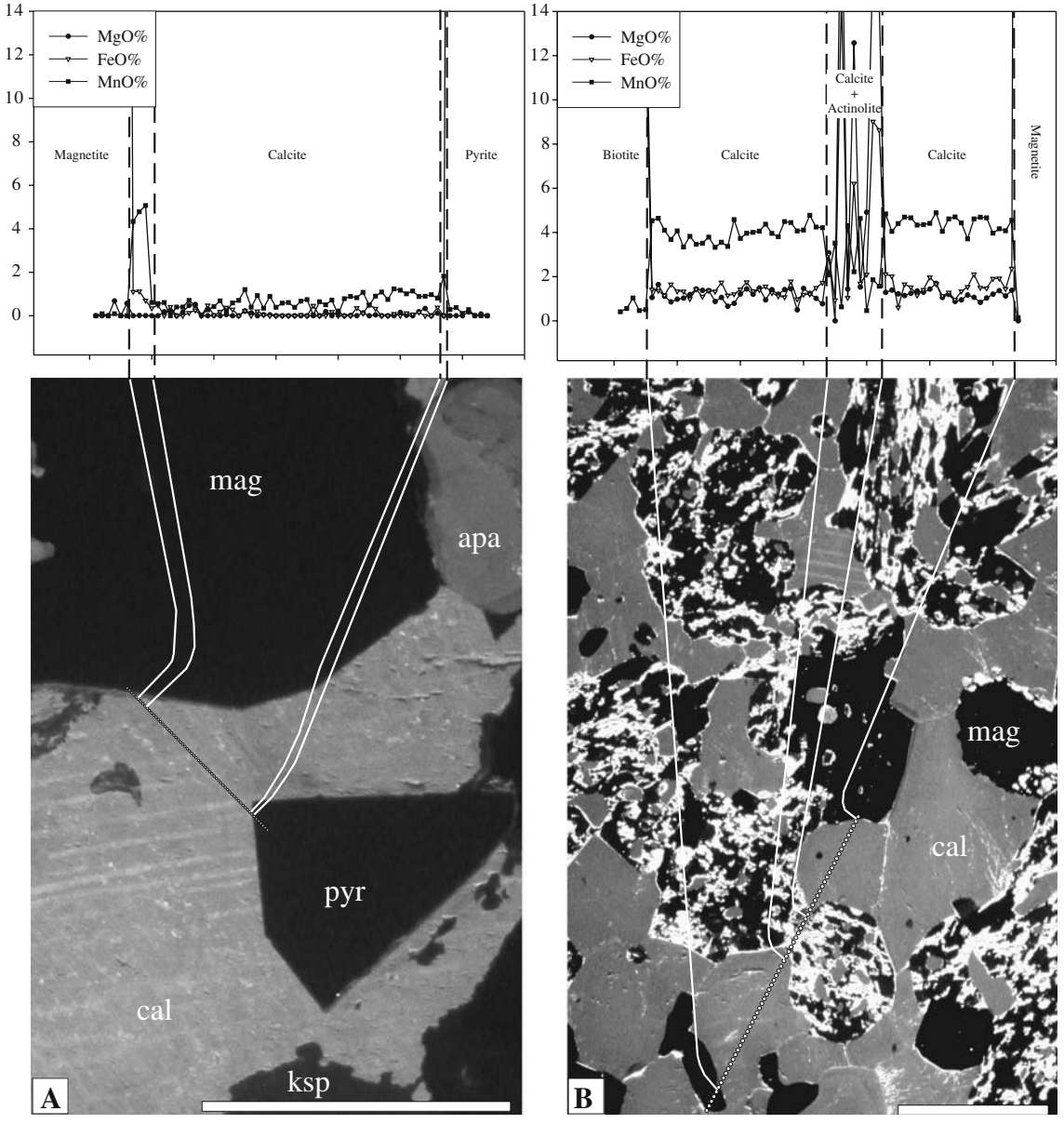

Fig. 7 CL images and microprobe traverses for calcite in **a** Ernest Henry ore breccia and **b** Ernest Henry marble matrix breccia. Note elevated MnO concentrations adjacent to magnetite grains. *Scale bars*=500 μm

quartz, pyrite, chlorite, albite, biotite, magnetite and hematite assemblages. Ore zones comprise tabular brecciated veins and fault zones up to 6 m in width. Veinlets and disseminated mineralisation occur between the main ore lodes (Cannell and Davidson 1998).

Mt Elliott deposit

Mt Elliott (Fig. 1) is a small Cu–Au deposit (2.9 Mt of 3.33% Cu and 1.47 g/t Au; Fortowski and McCracken 1998) hosted by schist, phyllite, andesite and amphibolite of the Kuridala Formation (Cover Sequence 3). The bulk of mineralisation is hosted by the 'outer carapace breccia', along and above the gently dipping reverse Jocks Fault. The outer carapace breccia lacks a significant matrix component, exhibits minor block rotation and grades downwards into a zone characterized by meter-scale dilational vugs between angular to subangular rotated breccia blocks (Little 1997). Open spaces in the breccia contain a skarn-like assemblage of extremely coarse magnetite–pyrite–chalcopyrite–pyrrhotite–calcite ± garnet, actinolite, titanite, epidote, biotite, hematite, albite, K-feldspar, chlorite and late gypsum. Individual mineral grains are commonly 5 to 100 cm in diameter.

Starra (Selwyn) deposit

Mineralisation in the Starra or Selwyn mining camp (Fig. 1) comprises a number of historic mines with a combined pre-mining global resource of 49 Mt at 1.76 g/t

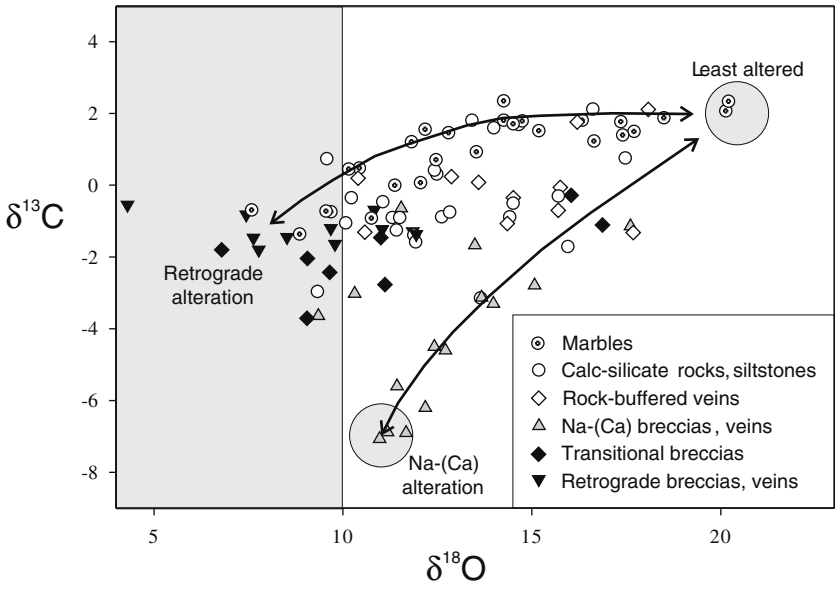

Fig. 8 Carbon and oxygen isotope data from the Cloncurry District record equilibration between unaltered marbles and calc-silicate rocks, and fluids responsible for albite–actinolite-rich alteration and retrograde chlorite-bearing alteration. *Arrows* represent observed data variations as opposed to model curves. Data are from this study and from Hingst (2002)

Au and 1.05% Cu (using a 1% Cu cut off; Sleigh 2002). Mineralisation is hosted by a series of tabular or lensoidal 'ironstone' bodies in a sequence of schist and calc-silicate rocks of the Staveley Formation (Cover Sequence 3). The origin of the ironstones has been contentious, with syngenetic (e.g. Davidson 1989) and epigenetic origins having been proposed. Rotherham (1997) interpreted the ironstone bodies to be the products of pervasive K–Fe (biotite–magnetite–hematite–quartz–pyrite) metasomatism and to be overprinted by a distinct hematite-rich mineralising phase (quartz–anhydrite–calcite–hematite–gold–pyrite–chalcopyrite–bornite–chalcocite–magnetite–chlorite–muscovite assemblage).

Osborne deposit

The Osborne deposit (15.2 Mt at 3.0% Cu and 1.05 g/t Au; Tullemans et al. 2001) is predominantly hosted by a sequence of feldspathic psammite, pelite and pegmatite of the Maronan Supergroup (Cover Sequence 3). Barren magnetite–quartz ironstones of debatable origin are common in the area and predate ore emplacement. Mineralisation is characterised by quartz–chalcopyrite–pyrite–pyrrhotite–magnetite bodies commonly with biotite–magnetite alteration selvages overprinted by sericite–chlorite–calcite alteration (Williams and Skirrow 2000).

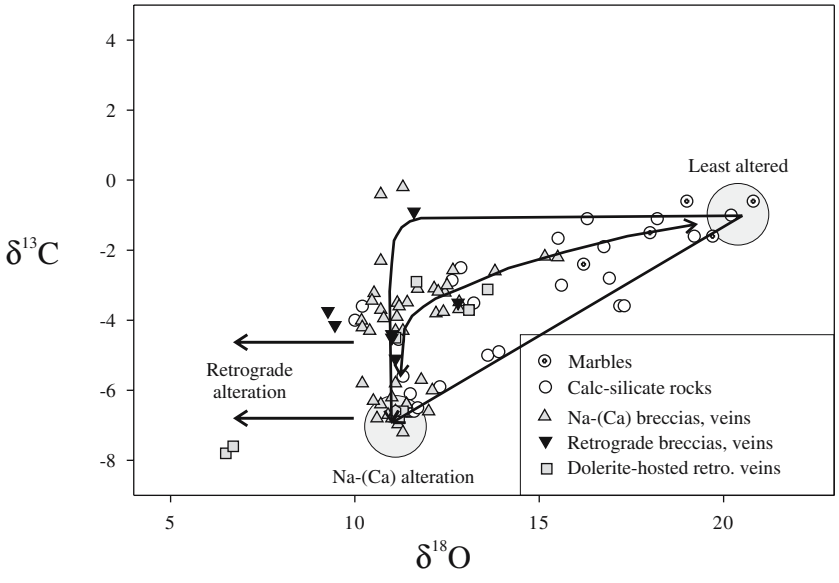

Fig. 9 Carbon and oxygen isotope data from late-metamorphic metasomatic systems in the MKFB record equilibration between unaltered marbles and calc-silicate rocks, and fluids responsible for albite–actinolite-rich alteration. Minor shifts to $\delta^{18}O$ values below ca. 10‰ are coincident with low-temperature mineral assemblages and record a distinct CO_2-poor, $\delta^{18}O$-depleted fluid source. *Arrows* represent observed data variations as opposed to model curves. Data are from Oliver et al. (1993) and this study

Carbon and oxygen stable isotopes

Cloncurry District

Isotopic data from Cloncurry District marbles form a curved array from approximately 20.5 to 8‰ $\delta^{18}O$ and 2 to −1‰ $\delta^{13}C$ (Fig. 8). Isotopic ratios notably vary significantly within individual hand specimens (range up to 6‰ $\delta^{18}O$ and 1‰ $\delta^{13}C$). The least-depleted isotope signatures are from samples that lack chlorite or actinolite, and isotopic values from these samples are consistent with little altered, metamorphosed Proterozoic marine carbonates (e.g. Valley 1986). Samples with the most depleted isotopic signatures contain significant chlorite and fine-grained hematite dusting of calcite. The large isotopic shifts and correspondence between depleted isotope signatures and abundance of chlorite and hematite suggest that isotopic variations can be largely attributed to fluid infiltration (e.g. Valley 1986).

Isotopic ratios for least-altered calc-silicate rocks range from approximately 17‰ $\delta^{18}O$ and 1.5‰ $\delta^{13}C$ to isotopically lighter ratios (Fig. 8). Where cut by veins and breccia bodies, calc-silicate rocks and meta-siltstones are progressively altered to albite–actinolite- or chlorite-rich mineral assemblages and show corresponding depletions in calcite $\delta^{18}O$ and $\delta^{13}C$ values as low as ca. 9 and −3‰, respectively (Fig. 8).

Isotopic analyses from rock-buffered veins overlap with analyses from least-altered marbles, calc-silicate rocks and meta-siltstones (Fig. 8).

Isotopic data are presented from calcite-bearing breccias and veins associated with high temperature (400–600°C) sodic–(calcic) alteration assemblages within Corella Formation stratigraphy of the Cloncurry District. Carbon and oxygen isotopic data form a distinct cluster at 11‰ $\delta^{18}O$ and −7‰ $\delta^{13}C$, with spread towards higher carbon and both higher and lower oxygen values (Fig. 8).

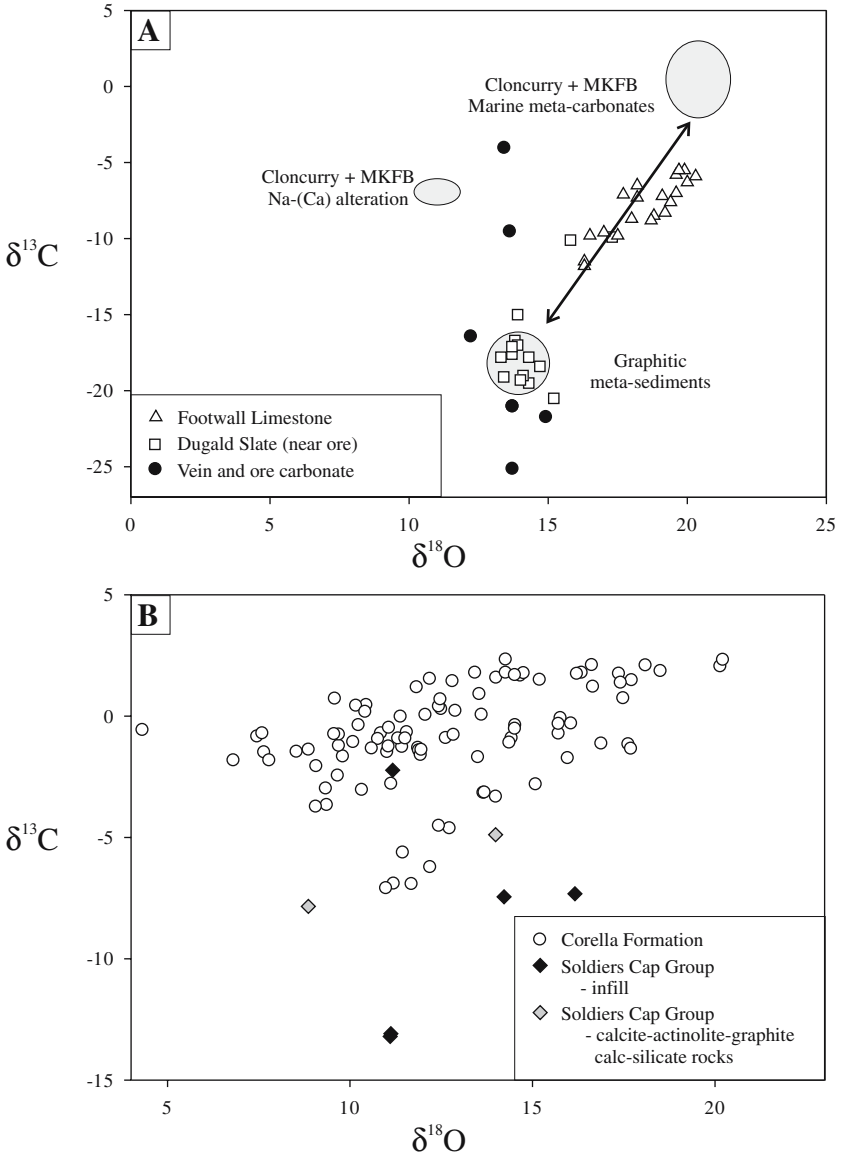

Fig. 10 **a** Isotopic data from the Dugald River Zn–Pb–Ag deposit define a linear array between graphitic meta-sedimentary and marine meta-carbonate host-rocks to the deposit. Veins and (remobilised?) ore samples may record an additional carbon and oxygen source. *Arrow* represents observed data variations as opposed to a model curve. Data are from Porter (1990) and Dixon and Davidson (1996). **b** Carbon and oxygen isotope data from carbonaceous lithologies and calcite breccia and vein infill within the Soldiers Cap Group of the Cloncurry District record distinctly low $\delta^{13}C$ values relative to samples within the Corella Formation. Data are from this study and from Hingst (2002)

Table 5 Ore deposit characteristics and isotopic ranges

Deposit	Host rocks	Mineralisation style	$\delta^{18}O$ (‰)	$\delta^{13}C$ (‰)
Ernest Henry	Cover Sequence 2: Mt Fort Constantine volcanics and marble matrix breccia	Milled breccia with K-feldspar, magnetite, carbonate, quartz, biotite, pyrite and chalcopyrite ore assemblage	1 to 21	−6 to 3
Great Australia	Cover Sequences 2 and 3: Toole Creek volcanics and adjacent Corella Formation meta-carbonate rocks	Tabular vein and fault zones with carbonate, actinolite, quartz, pyrite, chlorite, albite, biotite, magnetite and hematite ore assemblage	10 to 18	−16 to −3
Mt Elliott	Cover Sequence 3: Kuridala Formation schist, phyllite, andesite and amphibolite	Angular and vuggy breccia with coarse-grained, skarn-like (garnet, actinolite, diopside bearing) ore assemblage	11 to 13	−9 to −6
Starra	Cover Sequence 3: Staveley Formation schist, calc-silicate rocks and ironstone	Biotite and magnetite ironstone bodies overprinted by hematite-rich Cu–Au mineralisation	8 to 29	−17 to 1
Osborne	Cover Sequence 3: pelitic gneiss, schist, pegmatite and ironstone	Magnetite–quartz ironstone bodies overprinted by quartz–chalcopyrite–pyrite–pyrrhotite–magnetite ore assemblage	14 to 24	−7 to −4

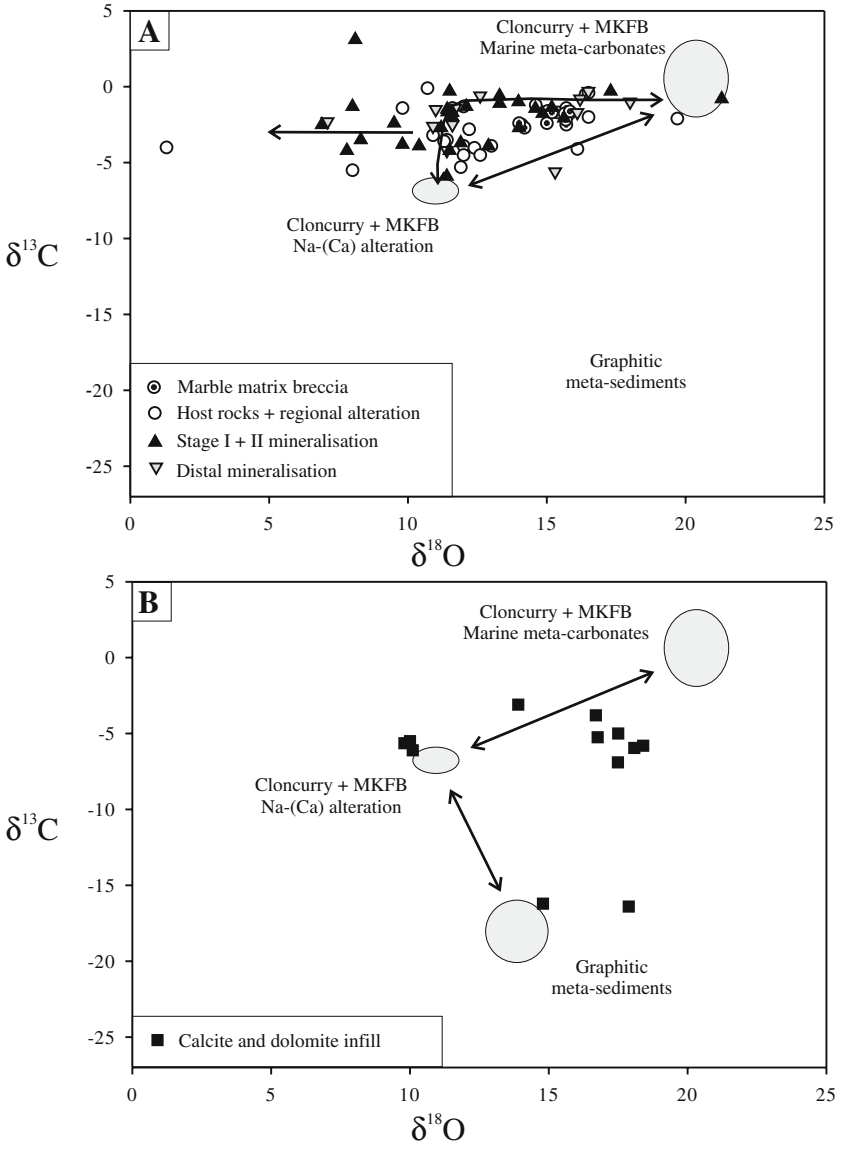

Fig. 11 **a** The bulk of the carbon and oxygen isotopic data from Ernest Henry is consistent with oxygen and carbon being sourced from Corella Formation marine meta-carbonates, and fluids similar to those responsible for regional sodic–(calcic) alteration. *L-shaped curves* imply that fluids were H_2O-rich but contained some CO_2. Shifts to $\delta^{18}O$ values below ca. 10‰ record a small component of isotopically light fluid. *Arrows* represent observed data variations as opposed to model curves. Data are from Twyerould (1997), Mark et al. (1999) and this study. **b** Isotope data from the Great Australia Cu–Au deposit record interaction between a fluid that is isotopically similar to that responsible for regional sodic–(calcic) alteration, marine meta-carbonates and graphitic meta-sediments. *Arrows* represent observed data variations as opposed to model curves. Data are from Davidson and Garner (1997) and Cannell and Davidson (1998). **c** Carbon and oxygen stable isotope data from Cu–Au deposits hosted within Cover Sequence 3 predominantly lies between fields defined for sodic–(calcic) alteration, marine meta-carbonates and graphitic meta-sediments. The Starra and Osborne ironstones define a separate trend, implying a distinct isotopic source. *Arrow* represents observed data variations as opposed to a model curve. Data sources are given in Table 2

Fig. 11 (continued)

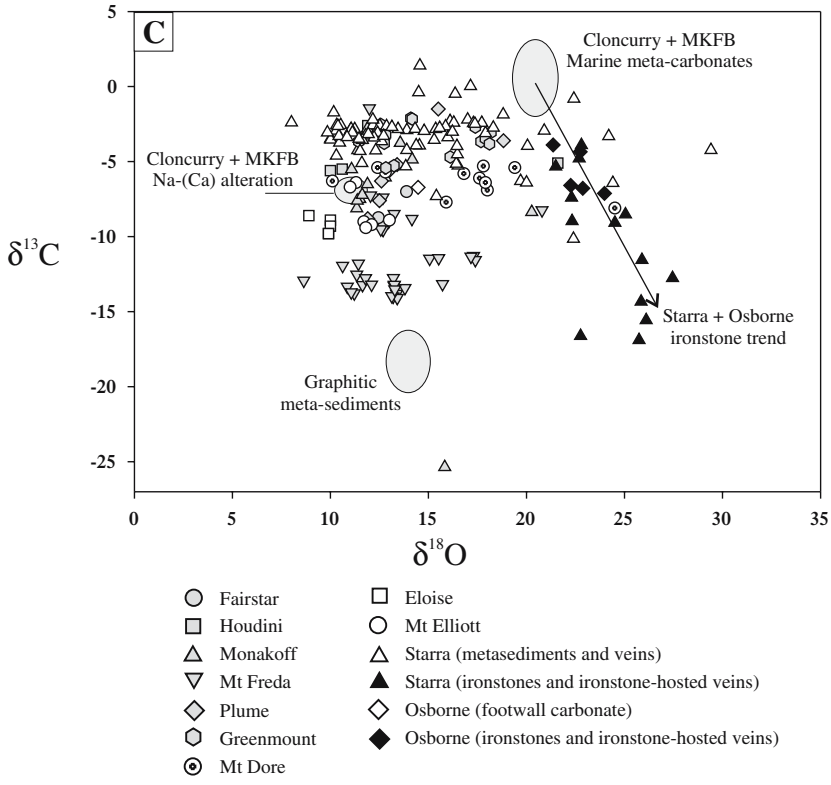

Retrograde breccias and veins define an array from approximately 4 to 12‰ $\delta^{18}O$ and approximately −0.7 to −1.6‰ $\delta^{13}C$ (Fig. 8). Isotopic data from transitional breccias and veins form an array that falls between the sodic–(calcic) and retrograde samples (Fig. 8).

Mary Kathleen fold belt

Carbon and oxygen isotope data from large-width, high-temperature (400–600°C), calcite-dominated veins and associated sodic–(calcic) alteration in Corella Formation marbles, calc-silicate rocks and meta-dolerites in the Mary Kathleen Fold Belt have been described by Oliver et al. (1993). Isotopic ratios from the cores of the large calcite veins cluster at ca. 11‰ $\delta^{18}O$ and −7‰ $\delta^{13}C$, while smaller calcite veins and altered breccias record isotopic ratios ranging up to ca. 15.5‰ $\delta^{18}O$ and −2‰ $\delta^{13}C$ (Fig. 9). Least-altered wallrocks record isotopic ratios of ca. 21‰ $\delta^{18}O$ and −1‰ $\delta^{13}C$. L-shaped trends in the isotopic data (Fig. 9) indicate that mixed H_2O–CO_2 metasomatic fluids were nonetheless oxygen-rich and carbon-depleted relative to the calcareous wallrocks.

Isotopic analyses of calcite from retrograde breccias and veins in the MKFB lack distinct clustering with respect to either $\delta^{18}O$ or $\delta^{13}C$ values. Most samples, however, record $\delta^{18}O$ signatures (ca. 6 to 10‰) that are depleted relative to the high-temperature veins described above (Fig. 9).

Carbonaceous meta-sedimentary rocks

Isotopic data from the carbonaceous hostrocks to the Dugald River Pb–Zn–Ag deposit (Dixon and Davidson 1996) define a linear array that can be divided into two endmember isotopic and geologic populations (Fig. 10a). Analyses from graphitic meta-sedimentary rocks at the ore horizon exhibit a tight data cluster at ca. 14‰ $\delta^{18}O$ and −18‰ $\delta^{13}C$. Analyses from the graphitic footwall limestone range from ca. 20‰ $\delta^{18}O$ and −5‰ $\delta^{13}C$ to ca. 16‰ $\delta^{18}O$ and −12‰ $\delta^{13}C$ and fall between data clusters defined above for graphitic meta-sedimentary rocks and marine meta-carbonate rocks. Analyses presented by Porter (1990) and Dixon and Davidson (1996) from vein and ore carbonates overlap with analyses from the near-ore Dugald Slates and extend to higher and slightly lower $\delta^{13}C$ values.

Additional samples including calcite–actinolite–graphite-rich calc-silicate rocks and breccia- and vein-infill hosted by graphitic meta-sedimentary rocks have been analysed from the Soldiers Cap Group (Cover Sequence 3), east of the town of Cloncurry. The samples record $\delta^{13}C$ values as low as −13.2‰ (Fig. 10b) that are distinctly depleted relative to samples from within the Corella Formation.

Cu–Au mineralisation

Isotopic ranges and key characteristics for select Cu–Au ore deposits are summarized in Table 5.

Cover Sequence 2: Ernest Henry deposit

Isotopic data presented here from the Ernest Henry deposit (166 Mt at 1.1% Cu and 0.55 g/t Au; Ryan 1998) are from Twyerould (1997), Mark et al. (1999) and this study. Isotopic data from the Ernest Henry deposit show a broad range in $\delta^{18}O$ values between ca. 1 and 21‰ and a comparatively narrower range in $\delta^{13}C$ values between ca. 3 and −6‰ (Fig. 11a). The bulk of the isotopic data falls between fields defined above for eastern Mt Isa Block marine meta-carbonate rocks and calcite in the cores of Na–(Ca) alteration systems. A subordinate amount of data extends to $\delta^{18}O$ values as low as 6‰ and for a single sample ca. 1‰.

Cover Sequences 2 and 3: Great Australia deposit

Isotopic data reported by Davidson and Garner (1997) and Cannell and Davidson (1998) from Great Australia show a wide range in both $\delta^{18}O$ and $\delta^{13}C$ ratios (Fig. 11b). A cluster of analyses at ca. 10‰ $\delta^{18}O$ and −6‰ $\delta^{13}C$ is similar to values at 11‰ $\delta^{18}O$ and −7‰ $\delta^{13}C$ for albite–actinolite-rich breccias and veins in both the Cloncurry District and MKFB. Another cluster at ca. 17.5‰ $\delta^{18}O$ and −5‰ $\delta^{13}C$ approaches values typical of little-altered marbles and calc-silicate rocks. Additional samples from Great Australia record depleted $\delta^{13}C$ values of ca. −16‰ that are similar to values recorded from graphitic meta-sedimentary rocks at the Dugald River deposit.

Cover Sequence 3: various deposits

Carbonate mineral carbon and oxygen stable isotope data are presented from numerous Cu–Au systems within Cover Sequence 3 of the eastern Mt Isa Block, including the Starra, Mt Elliott, Eloise, Osborne, Greenmount, Monakoff, Mt Freda and Mt Dore (Cu)–(Au) deposits, and the Fairstar, Houdini and Plume prospects. The data include analyses from altered and unaltered host rocks as well as metasomatic assemblages. The bulk of the data lies within a broadly triangular three-endmember field (Fig. 11c). Endmember ratios are similar to ratios defined above for (1) marine meta-carbonate rocks, (2) graphitic meta-sedimentary rocks and (3) calcite from the cores of sodic–(calcic) alteration systems. An exception to this distribution of data is evident in analyses from ironstones at the Starra and Osborne deposits which exhibit elevated $\delta^{18}O$ and depleted $\delta^{13}C$ values. Some deposits, most notably Mt Elliott, display little spread in data away from the field defined for sodic–(calcic) alteration.

Discussion

Implications of CL textures in calcite

From CL imagery, we recognize four principal calcite populations: (1) dull-luminescing metamorphic calcite in marbles and calc-silicate rocks, (2) moderate-luminescing calcite with weakly developed (or poorly preserved?) growth zoning in breccia and vein infill in sodic–(calcic) metasomatic assemblages as well as in the Ernest Henry ore breccia, (3) bright-luminescing calcite with well-developed growth zoning as infill in retrograde breccias and veins, and (4) networks of bright-luminescing calcite that overprint marble calcite, Ernest Henry ore calcite and calcite infill in sodic–(calcic) assemblages but which do not overprint retrograde assemblages.

Networks of bright-luminescing calcite similar to those noted in this study have been documented elsewhere by other researchers (e.g. Lewis et al. 1998) and interpreted to record metasomatic fluid pathways, along which calcite chemistry has been modified, resulting in the change in CL response. This interpretation is also preferred for samples

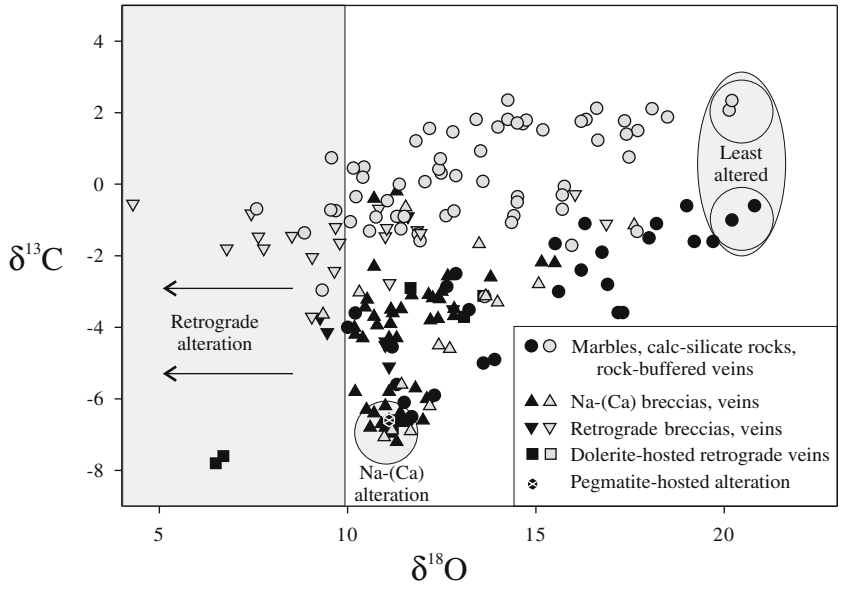

Fig. 12 Carbon and oxygen isotope data from regional host rocks and post-peak metamorphic alteration in the Corella Formation of the MKFB (*black symbols*) and Cloncurry District (*grey symbols*). Note the varying starting compositions for least-altered marbles and calc-silicates in the Cloncurry District vs the MKFB. Also note the coincident ratios for calcite associated with sodic–(calcic) alteration in both belts. Data are from Oliver et al. (1993), Hingst (2002) and the present study

analysed in this study, particularly given the associated chemical changes evident in the marble samples. A broad correspondence is noted between abundance of bright-luminescing calcite and the degree of depletion in $\delta^{18}O$ and $\delta^{13}C$ values for marble samples, further suggesting that fluid flow resulted in isotopic shifts in the samples. As such, the variability in isotopic signatures within individual marble samples is readily explained by the heterogeneous distribution of bright-luminescing calcite. These networks of bright-luminescing calcite must post-date any significant recrystallization of calcite grains during metamorphism and high-temperature deformation.

The preservation of growth banding in retrograde breccias and veins also indicates that calcite precipitation in these samples post-dates any significant recrystallization, indicating a late-tectonic timing for retrograde metasomatism. We postulate that retrograde breccias and veins (population 3 above) as well as networks of bright-luminescing calcite (population 4 above) can be attributed to a common, late-tectonic, low-temperature fluid flow event with fluids marked by low (<10‰ calcite) $\delta^{18}O$ signatures. This event clearly postdates ore genesis at Ernest Henry as well as the other higher-temperature regional breccias noted above.

Eastern Mt Isa Block C and O isotopic reservoirs

The bulk of the carbon and oxygen isotopic data collected from regional host rocks and post-peak metamorphic alteration assemblages in the Cloncurry District and Mary Kathleen Fold Belt can be described in terms of carbon and oxygen sourced from four main isotopic reservoirs, each of which has a distinct isotopic signature. These reservoirs are: (1) least-altered, marine meta-carbonate rocks, most common in the Corella and equivalent formations (Cover Sequence 2) but also represented locally in Cover Sequence 3 (e.g. Staveley Formation), (2) graphitic meta-sedimentary rocks most abundant in Cover Sequence 3 (e.g. Dugald Slates and the Soldiers Cap Group), (3) causative fluids for high-temperature, albite–actinolite-rich Na–(Ca) alteration, and (4) causative fluids for retrograde chlorite–hematite-bearing alteration.

Marine meta-carbonate rocks

In the Cloncurry District, least-altered marbles and calc-silicate rocks record isotopic ratios of ca. 20.5 ‰ $\delta^{18}O$ and 2‰ $\delta^{13}C$ (Fig. 12). In contrast, chemically similar (but with higher metamorphic grade), least-altered lithologies in the MKFB record isotopic ratios of ca. 20.5‰ $\delta^{18}O$ and −1‰ $\delta^{13}C$ (Fig. 12). The variation in $\delta^{13}C$ signatures may be attributed to either (1) primary variations in isotopic ratios, (2) greater degrees of metamorphic decarbonation in the amphibolite facies MKFB samples relative to the greenschist facies Cloncurry District samples, or (3) thermally driven isotopic equilibration between carbonates and reduced carbon, resulting in reduced $\delta^{13}C$ calcite values at higher metamorphic grade (e.g. Des Marais 2001).

Graphitic meta-sedimentary rocks

Data from the Dugald River deposit indicate $\delta^{13}C$ values of ca. −18‰ for carbonates within metamorphosed black shales (Fig. 10a). Graphite in this sequence has also been measured as −35.5 to −22.2‰ $\delta^{13}C$ (Dixon and Davidson 1996), consistent with an organic carbon origin. The depleted carbon isotopic ratios evident in samples from the Soldiers Cap Group (Fig. 10b) are interpreted to reflect partial equilibration between metasomatic fluids and graphitic meta-sedimentary rocks, which are common in this sequence. As such, $\delta^{13}C$ values reported here for veins within the Soldiers Cap Group (ca. −2 to −13‰ $\delta^{13}C$) appear to have been only partially buffered by the veins' immediate host rocks.

Causative fluids for Na–(Ca) alteration

Isotopic values for calcite associated with albite- and actinolite-rich sodic–(calcic) alteration in both the MKFB and Cloncurry District strongly cluster around the same value (Fig. 12). This, together with similarities in mineralogy, structural style and structural timing, suggests a widespread metasomatic event with a similar fluid source and similar fluid pathways in both the Cloncurry District and MKFB. Furthermore, the strong clustering of data at 11‰ $\delta^{18}O$ and −7‰ $\delta^{13}C$ indicates that, in the cores of the large sodic–(calcic) alteration systems, isotopic signatures were strongly fluid-buffered with respect to both $\delta^{18}O$ and $\delta^{13}C$. These values are clearly out of isotopic equilibrium with local wallrocks, requiring an externally derived fluid source. Isotopic ratios from the more distal portions of the alteration systems are increasingly more rock-buffered.

Causative fluids for retrograde alteration

Retrograde breccias and veins in the eastern Mt Isa Block record depleted $\delta^{18}O$ values (below ca. 10‰ $\delta^{18}O$) relative to other metasomatic associations (Fig. 12). These values cannot be explained by cooling (which would result in higher $\delta^{18}O$ calcite values) and are inferred to reflect input of an isotopically distinct fluid. In the available data sets, retrograde metasomatic assemblages are better represented in the Cloncurry District than in the MKFB (Fig. 12). While this may to some degree be a function of sampling bias, regional alteration mapping (Oliver, unpublished data, 1990; Marshall 2003) confirms that retrograde alteration assemblages are far more widespread in the Cloncurry District than in the MKFB.

Metasomatic fluid sources

One of the principal arguments that has been used to discount magmatic fluid sources for sodic–(calcic) alteration and iron-oxide–copper–gold mineralisation has been that the isotopic signatures of metasomatic fluids equilibrate with wallrocks along fluid flow paths, rendering interpretation of fluid sources ambiguous (e.g. Haynes 2000). With respect to sodic–(calcic) alteration in the eastern Mt Isa Block, although shifts are noted towards progressively more rock-buffered isotopic ratios as well as isotopically lighter $\delta^{18}O$ values, there is a strong clustering of data at 11‰ $\delta^{18}O$ and −7‰ $\delta^{13}C$ (Fig. 12). The degree of clustering of isotopic ratios indicates an isotopically homogenous fluid.

In the eastern Mt Isa Block, meta-sedimentary rocks in both Cover Sequences 2 and 3 are out of isotopic equilibrium with the fluid of interest, precluding the possibility of a metamorphic fluid source derived from these tectonostratigraphic sequences. Alternatively, isotopic values for calcite in sodic–(calcic) assemblages are consistent with those expected for igneous rocks (e.g. Valley 1986) and may indicate that either (1) fluids of a non-magmatic source were thoroughly equilibrated with magmatic rocks or (2) fluids were exsolved from crystallising intrusive bodies. However, with the exception of carbonatites which are not present in the Mt Isa Block, CO_2 concentrations in magmas are typically low, and the majority of this is released into hydrothermal fluids during crystallisation, with relatively little carbon incorporated into igneous rocks (e.g. Baker 2002). As a result, it is not possible to explain the buffering of the $\delta^{13}C$ signature of metasomatic fluids by crystalline igneous rocks in the eastern Mt Isa Block, particularly for fluids that have been shown to contain significant CO_2 through fluid inclusion studies (e.g. de Jong and Williams 1995). In contrast, crystallizing plutons in the eastern Mt Isa Block have been documented to exsolve CO_2–H_2O-rich fluids (e.g. Mark and Foster 2000; Perring et al. 2000) and represent the most probable fluid source for Na–(Ca) alteration (see also Pollard 2001; Oliver et al. 2004).

In the Cloncurry District, some rocks record low $\delta^{13}C$ signatures, reflecting a contribution from organic carbon reservoirs of black shales (Fig. 10). In theory, it may be possible to produce the carbon isotope values in regional sodic–(calcic) alteration by admixture of marine carbon with organic carbon. However, this possibility is not supported by the strong clustering of data from Na–(Ca)-rich assemblages around −7‰ $\delta^{13}C$, which suggests a single reservoir rather than a mixed one.

Retrograde, chlorite-bearing metasomatic assemblages display low $\delta^{18}O$ values. A spread in $\delta^{13}C$ values indicates that retrograde fluids were relatively CO_2-poor (e.g. Valley 1986), and this has been confirmed by preliminary fluid inclusion work (Fu, in preparation) The relatively low temperature (i.e. chlorite-stable), low $\delta^{18}O$ signature and low CO_2 content of these fluids are consistent with a meteoric origin. A lack of distinct clustering in $\delta^{18}O$ values suggests that either the fluids equilibrated to varying degrees with host lithologies or were mixed with fluids from other sources. The recognition of breccias and veins with ‘transitional’ actinolite ± epidote ± chlorite mineralogy in regional alteration assemblages may record mixing between saline, high-temperature (magmatic) and dilute, low-temperature (meteoric) fluids. Preliminary fluid inclusion data (Fu, in preparation) are consistent with this hypothesis.

Requisite fluid volumes

We have demonstrated examples of both predominantly fluid-buffered (e.g. Mt Elliott Cu–Au) and increasingly rock-buffered (e.g. Ernest Henry Cu–Au) metasomatic assemblages in the eastern Mt Isa Block. No attempt has been made to estimate the relative abundance of these two endmember assemblages, and such an estimate would be tenuous given (1) the extreme heterogeneity of isotopic resetting from district to microscopic scales (as inferred from map, hand specimen and CL observations), (2) the inherent difficulty in estimating the degree of isotopic resetting at outcrop and district scale, and (3) the inherent sampling bias towards visibly altered rocks. These difficulties can be avoided in making a simplifying assumption that an ‘average-altered rock’ has an isotopic signature that is midway between fluid- and rock-buffered signatures. Such an average would take into account the occurrence of both more fluid- and rock-buffered assemblages.

To produce a hypothetical ‘average-altered rock’, an unaltered rock would need to be completely equilibrated with a volume of fluid containing the same number of atoms of the element of interest (e.g. C or O) as contained in the rock. For example, a kilogram of pure calcite marble ($CaCO_3$) contains some 1.80×10^{22} oxygen atoms and 6.01×10^{21} carbon atoms and would have to equilibrate with the same number of oxygen and carbon atoms in a metasomatic fluid to produce an ‘average-altered rock’.

We have argued that the most likely source for causative fluids for Na–(Ca) alteration in the eastern Mt Isa Block is via exsolution from crystallizing intrusive rocks. As indicated by Pollard (2001), magma water contents of 4.5–6.5 wt% are likely for the Williams and Naraku intrusions. Assuming 4 wt% fluid exsolution and inferred fluid compositions of 40 wt% Na + K salts, 20 wt% CO_2 and 40 wt% H_2O (e.g. Oliver et al. 2004), each kilogram of magma would exsolve 0.04 kg of fluid containing some 4.89×10^{20} oxygen atoms and 1.22×10^{20} carbon atoms. As such, 1 kg of magma could exsolve enough fluid to reset 0.020 kg of pure calcite marble to ‘average-altered’ carbon isotopic values (or reset 0.027 kg of calcite to ‘average-altered’ oxygen isotopic values).

The Williams batholith crops out over approximately 2,100 km^2 in the southern portion of the eastern Mt Isa Block. Assuming comparable depth extents to outcropping intrusive rocks and altered rocks, fluids exsolved from outcropping regions of the Williams batholith would have been capable of resetting the carbon isotopic signature of greater than 40 km^2 of pure calcite marble or greater than

800 km^2 of metamorphic rocks with an average calcite content of 5%. Although we have not specifically taken into account other carbonate species or graphite, our calculations suggest that the Williams batholith exsolved sufficient fluid produce the ~200 km^2 of sodic–(calcic) altered rocks in the southern portion of the eastern Mt Isa Block (e.g. Pollard 2001). Because of the ambiguity involved in balancing for a large number of oxygen-bearing mineral species, we have not attempted to repeat such calculations balancing for oxygen. We note, however, from curved isotopic arrays (e.g. Figs. 8 and 9) that rock oxygen isotopic signatures were more readily reset during alteration than the carbon signatures and, as such, carbon content of the metasomatic fluids was the limiting component in resetting metamorphic isotopic signatures.

Ore deposit isotope systematics

Most data from the Cu–Au ore systems lie within a three-endmember mixing array defined by values for eastern Mt Isa Block marine meta-carbonate rocks, graphitic meta-sedimentary rocks and sodic–calcic alteration of likely magmatic–hydrothermal origin. This suggests that ore fluids had a similar isotopic composition to that defined for causative fluids for sodic–(calcic) alteration and that isotopic variations in the deposit data can be explained by varying degrees of equilibration between such a fluid and marine meta-carbonate and graphitic meta-sedimentary rocks. Perhaps the best example of this is from the Great Australia deposit, which is hosted by Soldiers Cap Group lithologies but at a fault contact with the Corella Formation. Isotopic data from this deposit record shifts from values typical of sodic–(calcic) alteration towards values defined for marine meta-carbonate and graphitic meta-sedimentary rocks common in the Soldiers Cap Group and Corella Formation, respectively. As argued above for sodic–(calcic) metasomatic fluids, δ^{13}C values from the ore deposit data suggest that ore fluids were exsolved from crystallising intrusive rocks, as opposed to fluids of non-magmatic origins that were equilibrated with igneous rocks.

Carbon and oxygen isotope data from the Mt Elliott Cu–Au deposit cluster very close to values characteristic of sodic–(calcic) alteration systems (Fig. 11c). This, as well as similarities in mineral assemblages, suggests that fluids responsible for district-scale sodic–(calcic) alteration and Mt Elliott-style Cu–Au mineralisation were derived from similar sources and that the cores of these systems were strongly fluid-buffered. Minor shifts towards lower δ^{13}C

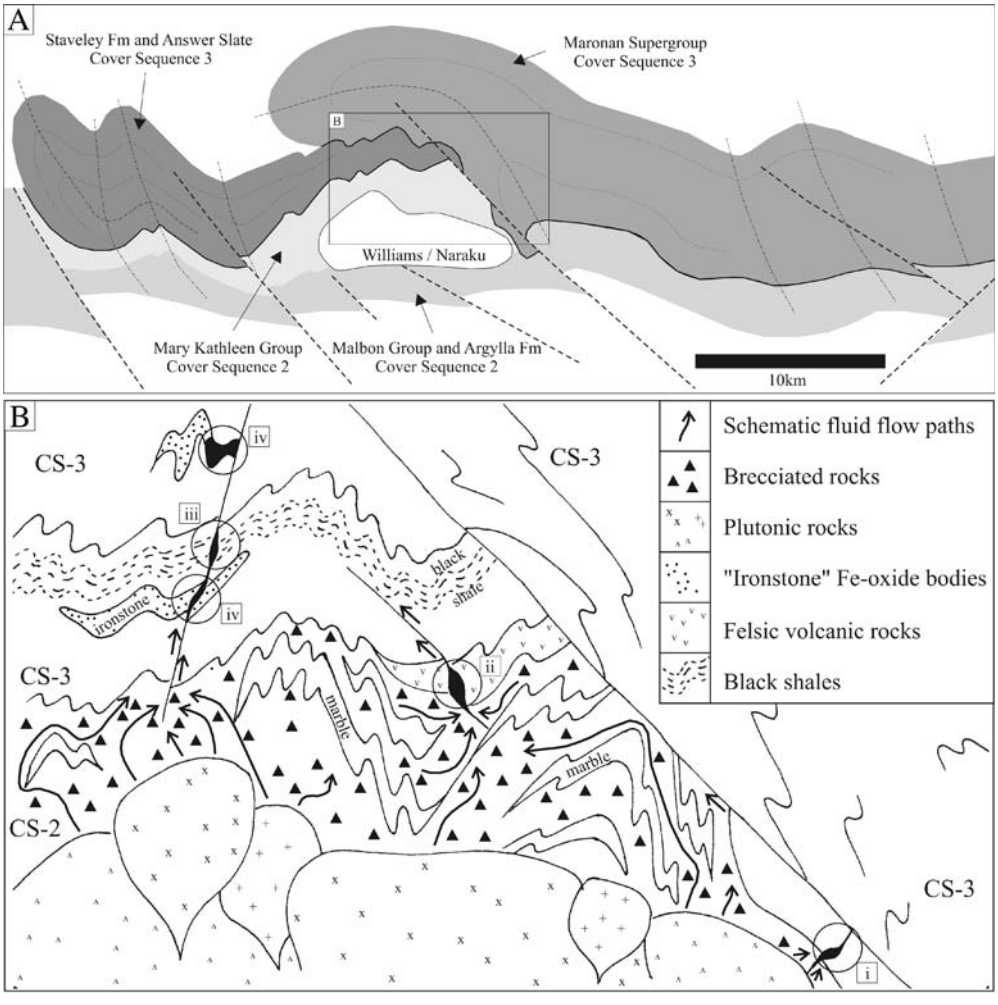

Fig. 13 **a** Schematic E–W cross-section of the Cloncurry District, modified after Giles and MacCready (1997). **b** Enlargement of an area indicated in **a** schematically illustrating the setting of various styles of late metamorphic Cu–Au mineralisation in the Cloncurry District. Intrusion-proximal, Mt Elliott-style deposits (*i*) record isotopic signatures similar to the fluid-buffered cores of Na–(Ca) alteration systems. Intrusion-distal deposits (*ii*, *iii* and *iv*) record a wide range in isotopic values, reflecting varying degrees of wallrock equilibration before mineralisation. Structural and stratigraphic hosts include thick sequences of relatively brittle rocks (e.g. felsic volcanic rocks: V pattern) as at the Ernest Henry deposit (*ii*), reduced stratigraphic sequences as at the Eloise deposit (*iii*) and pre-mineralisation ironstones, as at the Starra deposit (*iv*). *Arrows* represent possible fluid flow paths pre- and syn-mineralisation and reflect how widespread brecciation (*triangle pattern*) in the Corella Formation allowed fluids access to large volumes of rock. *CS-2*, Cover Sequence 2; *CS-3*, Cover Sequence 3

values and slightly higher $\delta^{18}O$ values in the Mt Elliott data record minor equilibration with graphitic meta-sedimentary rocks, which is also a feature of the S isotope systematics (Davidson and Dixon 1992).

Mineralisation at Starra is hosted by magnetite-rich ironstones that pre-date introduction of Au and Cu (e.g. Rotherham 1997). Williams et al. (2001) documented fluid chemistries that differ markedly between the ironstones and Cu–Au mineralisation and suggested that several distinct metasomatic fluids are recorded at the deposit. The majority of Br/Cl ratios reported by Williams et al. (2001) for the ironstones notably fall outside of fields defined for modern magmatic fluids.

The bulk of carbon and oxygen isotope data from both mineralised and barren veins and meta-sedimentary rocks at the Starra deposit lies between fields defined for marine meta-carbonates and calcite from sodic–(calcic) alteration assemblages (Fig. 11c). Thus, Au–Cu mineralisation at Starra can be explained by precipitation from metasomatic fluids that were isotopically similar to those responsible for sodic–(calcic) alteration but that equilibrated to varying degrees with carbonate-bearing meta-sedimentary rocks. In contrast, data from ironstones and some ironstone-hosted veins at the Starra and Osborne deposits extend from values in equilibrium with marine meta-carbonate rocks to higher $\delta^{18}O$ and lower $\delta^{13}C$ values (Fig. 11c). Davidson and Davis (2001) invoked reaction between CO_2–SO_4-rich fluids and the pre-existing ironstones to produce CH_4–H_2S-bearing reduced fluids that may explain the depleted $\delta^{13}C$ values evident at Starra and Osborne.

Recent geochronological and petrographic data suggest that iron oxide and Cu–Au mineralisation at Osborne occurred at ca. 1595 Ma (Gauthier et al. 2001; Rubenach et al. 2001), synchronous with the peak of metamorphism. No voluminous intrusions of this age are known in the eastern Mt Isa Block, and a metamorphosed (diagenetic?) or metamorphogenic origin for some ironstones at Osborne and Starra seems plausible, dissimilar to other ironstones with apparently more igneous-related affinity.

Some ore deposit data, particularly from the Ernest Henry deposit, fall at $\delta^{18}O^{calcite}$ values below −11‰ (Fig. 11a). As such, a meteoric fluid component cannot be ruled out and, indeed, such a source is invoked above for retrograde (chlorite–hematite) alteration in the MKFB and Cloncurry District. However, it has been shown through stable isotopes and CL images that Cloncurry District marbles record late-tectonic, low-temperature fluid flow that resulted in the depletion of $\delta^{18}O$ calcite values as low as 5‰. CL images of Ernest Henry samples also record similar late-tectonic, post-mineralisation fluid flow that may have also resulted in a shift to lower $\delta^{18}O$ values. Thus, while it seems likely that an isotopically light fluid, possibly of meteoric origin, is recorded by some of the Ernest Henry samples, at least some, if not all, of this fluid flow post-dates mineralisation.

Conclusions

The data presented in this contribution support a predominantly magmatic fluid source for both regional Na–(Ca) alteration and Cu–Au mineralisation in the eastern Mt Isa Block. Metamorphic fluid sources for most alteration and mineralisation assemblages are not consistent with the established isotopic signatures of the main meta-sedimentary host sequences. Furthermore, non-magmatic fluids isotopically equilibrated with igneous rocks cannot readily explain the $\delta^{13}C$ signatures of either Na–(Ca) alteration or Cu–Au mineralisation.

As a result of complex flow paths (Fig. 13), there is no clear $\delta^{13}C$ or $\delta^{18}O$ isotopic vector towards eastern Mt Isa Block Cu–Au mineralisation. Many syn-Cu–Au mineralisation carbonates record shifts in isotopic ratios towards those of their immediate and broader-scale host sequences, recording modification of fluid chemistry via fluid–wallrock interaction. Such interaction may account for the K- and Fe-rich nature of ore-proximal alteration in deposits that are distal to postulated igneous fluid sources. This is particularly noted for the Ernest Henry deposit. In contrast to Ernest Henry, data from some other deposits, most notably Mt Elliott, do not record significant shifts in isotopic ratios and, for this deposit, wallrock interaction does not appear to have been a necessary precursor to Cu–Au mineralisation.

Low-temperature, CO_2-poor, $\delta^{18}O$-depleted fluids of probable meteoric origin are involved in late stages of regional alteration but have not contributed significantly to the oxygen and carbon budgets in the Cu–Au ore environments. As such, meteoric fluids do not appear to have played a significant role in the genesis of most eastern Mt Isa Block Cu–Au mineralisation.

Whereas Starra Au–Cu mineralisation is largely consistent with a magmatic fluid source, pre-mineralisation ironstones from the Starra deposit and some magnetite alteration at Osborne record distinct isotopic ratios that are inconsistent with a magmatic fluid source. This indicates the potential of ironstones of other origins (apart from magmatic–hydrothermal) in acting as suitable chemical hosts for Cu–Au mineralisation.

Acknowledgements This contribution stems from a Ph.D. research by LJM at James Cook University, funding for which was provided by JCU and the pmd*CRC. Logistical support was provided by MIM Exploration (now Xstrata Copper Australia). Ernest Henry Mining arranged access to drill core at the Ernest Henry deposit. The samples for isotopic analyses from the Mt Elliott and Eloise deposits are from the JCU research sample collection. Unpublished analyses from the Starra and Osborne deposits were collected by GJD. Geordie Mark is thanked for allowing the use of recent data from the Ernest Henry deposit. Ian Cartwright (Monash University) undertook the majority of new (and many of the previously published) isotopic analyses. Hans Machel and Jeff Lonnee (University of Alberta) are thanked for assistance with CL equipment. Kevin Blake (JCU) assisted with microprobe analyses. The interpretation of the data has benefited from input by Tim Baker, Ian Cartwright, Bin Fu, Greg Dipple, Geordie Mark, Andrew McCaig, Mike Roberts, Bruce Yardley and others. The comments on earlier versions of the manuscript by Derek Thorkelson, Stephen Cox and Louise Corriveau and constructive reviews by Richard Naslund and an anonymous reviewer are gratefully acknowledged.

References

Baker T (2002) Emplacement depth and carbon dioxide-rich fluid inclusions in intrusion-related gold deposits. Econ Geol 97:1111–1117

Baker T, Perkins C, Blake KL et al (2001) Radiogenic and stable isotope constraints on the genesis of the Eloise Cu–Au deposit, Cloncurry District, Northwest Queensland. Econ Geol 96:723–742

Barton MD, Johnson DA (1996) Evaporitic-source model for igneous-related Fe oxide–(REE–Cu–Au–U) mineralization. Geology 24:259–262

Beardsmore TJ (1992) Petrogenesis of Mount Dore-style breccia-hosted copper + gold mineralisation in the Kuridala–Selwyn region of northwestern Queensland. Ph.D. thesis, James Cook University, Townsville, Australia

Blake DH (1987) Geology of the Mt Isa Inlier and environs, bulletin 225. Bureau of Mineral Resources, Geology and Geophysics, Canberra

Cannell J, Davidson GJ (1998) A carbonate-dominated copper–cobalt breccia–vein system at the Great Australia deposit, Mount Isa Eastern Succession. Econ Geol 93:1406–1421

Davidson GJ (1989) Starra and Trough Tank, iron-formation-hosted gold–copper deposits of north-west Queensland, Australia. Ph. D. thesis, University of Tasmania, Hobart

Davidson GJ, Davis BK (2001) Some controls on oxidation state variation of oxide Cu–Au systems. Geol Soc Am Abstr Prog 33 (6):2

Davidson GJ, Dixon GH (1992) Two sulphur isotope provinces deduced from ores in the Mount Isa Eastern Succession, Australia. Miner Depos 27:30–41

Davidson GJ, Garner A (1997) Advances in the understanding of the Cloncurry Cu–Au field. In: Pollard PJ (ed) AMIRA P438: Cloncurry base metals and gold final report. Australian Mineral Industry Research Association, Townsville, pp 14-1–14-11

de Jong G, Williams PJ (1995) Giant metasomatic system formed during exhumation of mid-crustal Proterozoic rocks in the vicinity of the Cloncurry fault, northwest Queensland. Aust J Earth Sci 42:281–290

Des Marais DJ (2001) Isotopic evolution of the biogeochemical carbon cycle during the Precambrian. In: Valley JW, Cole DR (eds) Stable isotope geochemistry reviews in mineralogy and geochemistry, 43. Mineralogical Society of America, Washington, pp 555–578

Dixon G, Davidson GJ (1996) Stable isotope evidence for thermo-chemical sulfate reduction in the Dugald River (Australia) strata-bound shale-hosted zinc–lead deposit. Chem Geol 129:227–246

Farmer GL, De Paulo DJ (1997) Sources of hydrothermal components:heavy isotopes. In: Barnes HL (ed) Geochemistry of hydrothermal ore deposits, 3rd edn. Wiley, New York, pp 31–62

Fletcher C (1999) Geology, mineralization and metamorphism of the Plume prospect, Northwest Queensland. BSc (Honours) thesis, James Cook University, Townsville

Fortowski DB, McCracken SJA (1998) Mount Elliott copper–gold deposit. In: Berkman DA, Mackenzie DH (eds) Geology of Australian and Papua New Guinean deposits, AUSIMM monograph 22. Australian Institute of Mining and Metallurgy, Melbourne, pp 775–781

Gauthier L, Hall G, Stein H et al (2001) The Osborne deposit, Cloncurry District: a 1595 Ma Cu–Au skarn deposit. In: Williams PJ (ed) A hydrothermal odyssey extended conference abstracts—EGRU contribution 59. Economic Geology Research Unit, Townsville, pp 58–59

Giles D, MacCready T (1997) The structural and stratigraphic position of the Soldiers Cap Group in the Mount Isa Inlier. In: Ailleres L, Betts P (eds) Structural elements of the Eastern Successions, a field guide illustrating the structural geology of the eastern Mount Isa terrane, Australia. Australian Geodynamics Cooperative Research Centre, Melbourne, pp 61–73

Giles D, Nutman AP (2002) SHRIMP U–Pb monazite dating of 1600–1580 Ma amphibolite facies metamorphism in the southeastern Mt Isa Block, Australia. Aust J Earth Sci 49:455–466

Golyshev SI, Padalko NL, Pechenkin SA (1981) Fractionation of stable isotopes in carbonate systems. Geochem Int 10:85–99

Hand M, Rubatto D (2002) The scale of the thermal problem in the Mt Isa Inlier. In: Preiss VP (ed) Geoscience 2002: expanding horizons. Abstracts of the 16th Australian Geological Convention. Geological Society of Australia, Adelaide, pp 173

Haynes DW (2000) Iron oxide copper (–gold) deposits: their position in the ore spectrum and modes of origin. In: Porter TM (ed) Hydrothermal iron-oxide copper–gold & related deposits: a global perspective. Australian Minerals Foundation, Adelaide, pp 71–90

Haynes DW, Cross KC, Bills RT, Reed MH (1995) Olympic Dam ore genesis: a fluid mixing model. Econ Geol 90:281–307

Hingst R (2002) Geology and geochemistry of the Cloncurry Fault, north-west Queensland, Australia. BSc (Honours) thesis, James Cook University, Townsville

Krcmarov RL (1995) Proterozoic geology and mineralisation of the Greenmount Cu–Au–Co deposit, Cloncurry District. MSc thesis, University of Tasmania, Hobart

Lewis S, Holness M, Graham C (1998) Ion microprobe study of marble from Naxos, Greece: grain-scale fluid pathways and stable isotope equilibration during metamorphism. Geology 26:935–938

Little GA (1997) Structural evolution and paragenesis of alteration and mineralisation at the Mount Elliott Cu–Au mine, Northwest Queensland. BSc (Honours) thesis, James Cook University, Townsville

Mark G, Crookes RA (1999) Epigenetic alteration at the Ernest Henry Fe-oxide–(Cu–Au) deposit, Australia. In: Stanley et al (eds) Mineral deposits: processes to processing. Society for Geology Applied to Mineral Deposits (SGA), London, pp 185–188

Mark G, Foster DRW (2000) Magmatic–hydrothermal albite–actinolite–apatite-rich rocks from the Cloncurry District, NW Queensland, Australia. Lithos 51:223–245

Mark G, Oliver NHS, Williams PJ, Crookes R, Valenta R, Gow P (1999) Characteristics and origins of the Ernest Henry iron oxide–copper–gold hydrothermal system: results of the 1999 Collaborative SPIRT research project. James Cook University, Townsville

Marshall LJ (2003) Brecciation within the Mary Kathleen Group of the Eastern Succession, Mt Isa Block, Australia: implications of district-scale structural and metasomatic processes for Fe-oxide–Cu–Au mineralisation. Ph.D. thesis, James Cook University, Townsville

McCrae JM (1950) On the isotope chemistry of carbonates and a paleotemperature scale. J Chem Phys 18:849–857
Newberry SP, Carswell JT, Allnutt SL et al (1993) The Dugald River zinc–lead–silver deposit: an example of a tectonised Proterozoic stratabound sulphide deposit. In: Matther I (ed) World zinc '93, AUSIMM publication series, v7. Australian Institute of Mining and Mettalurgy, Melbourne, pp 7–21
O'Dea MG, Lister GS, MacCready T et al (1997) Geodynamic evolution of the Proterozoic Mount Isa terrain. In: Burg J-P, Ford M (eds) Orogeny through time. Geological Society special publication no. 121, London, pp 99–122
O'Neil JR, Clayton RN, Mayeda TK (1969) Oxygen isotope fractionation in divalent metal carbonates. J Chem Phys 51:5547–5558
Ohmoto H, Rye RO (1979) Isotopes of sulphur and carbon. In: Barnes HL (ed) Geochemistry of hydrothermal ore deposits. Wiley, New York, pp 509–567
Oliver NHS, Wall VJ, Cartwright I (1992) Internal control of fluid composition in amphibolite–facies scapolitic calc-silicates, Mary Kathleen, Australia. Contrib Mineral Petrol 111: 94–112
Oliver NHS, Cartwright I, Wall VJ et al (1993) The stable isotope signature of kilometre-scale fracture-dominated metamorphic fluid pathways, Mary Kathleen, Australia. J Metamorph Geol 11:705–720
Oliver NHS, Mark G, Pollard PJ et al (2004) Geochemistry and geochemical modelling of fluid–rock interaction in the eastern Mt Isa Block, Australia: the role of sodic alteration in the genesis of iron oxide–copper–gold deposits. Econ Geol 99:1145–1176
Page RW, Sun S-S (1998) Aspects of geochronology and crustal evolution in the Eastern Fold Belt, Mt Isa Inlier. Aust J Earth Sci 45:343–361
Perring CS, Pollard PJ, Dong G et al (2000) The lightning creek sill complex, Cloncurry District, Northwest Queensland: a source of fluids for Fe oxide Cu–Au mineralization and sodic–calcic alteration. Econ Geol 95:1067–1089
Pollard PJ (2001) Sodic(–calcic) alteration in Fe-oxide–Cu–Au districts: an origin via unmixing of magmatic H_2O–CO_2–NaCl + –$CaCl_2$–KCl fluids. Miner Depos 36:93–100
Porter S (1990) The Dugald River lead–zinc deposit. BSc (Honours) thesis, University of Queensland, Brisbane
Rotherham JF (1997) A metasomatic origin for the iron-oxide Au–Cu Starra orebodies, Eastern Fold belt, Mount Isa Inlier. Miner Depos 32:205–218
Rotherham JF, Blake KL, Cartwright I et al (1998) Stable isotope evidence for the origin of the Mesoproterozoic Starra Au–Cu deposit, Cloncurry District, northwest Queensland. Econ Geol 93:1435–1449
Rubenach M, Adshead N, Oliver NHS et al (2001) The Osborne Cu–Au deposit: geochronology, and genesis of mineralization in relation to host albitites and ironstones. In: Williams PJ (ed) A hydrothermal odyssey, extended conference abstracts, EGRU Contribution 59. Economic Geology Research Unit, Townsville, pp 172–173
Ryan AJ (1998) Ernest Henry copper–gold deposit. In: Berkman DA, Mackenzie DH (eds) Geology of Australian and Papua New Guinean deposits, AUSIMM monograph 22. Australian Institute of Mining and Metallurgy, Melbourne, pp 759–768
Sleigh DWW (2002) The Selwyn line tabular iron–copper–gold system, Mount Isa Inlier, NW Queensland, Australia. In: Porter TM (ed) Hydrothermal iron-oxide copper–gold & related deposits: a global perspective, vol 2. Australian Mineral Foundation, Adelaide, pp 77–93
Thorkelson DJ, Mortensen JK, Davidson GJ et al (2001) Early Mesoproterozoic intrusive breccias in Yukon, Canada: the role of hydrothermal systems in reconstructions of North America and Australia. Precambrian Res 11:31–55
Tullemans FJ, Agnew P, Voulgaris P (2001) The role of geology and exploration within the mining cycle at the Osborne Mine, northwestern Queensland. In: Edwards AC (ed) Mineral resource and ore reserve estimation: the AusIMM guide to good practice. Australiasian Institute of Mining and Metallurgy, Carlton, pp 157–168
Twyerould SC (1997) The geology and genesis of the Ernest Henry Fe–Cu–Au deposit, Northwest Queensland, Australia. Ph.D. thesis, University of Oregon
Valley JW (1986) Stable isotope geochemistry of metamorphic rocks. In: Valley JW, Taylor HP, O'Neil JR (eds) Stable isotopes in high temperature geological processes, reviews in mineralogy, vol 16. Mineralogical Society of America, Washington, pp 445–489
Wang S, Williams PJ (2001) Geochemistry and origin of Proterozoic skarns at the Mount Elliott Cu–Au(–Co–Ni) deposit, Cloncurry District, NW Queensland, Australia. Miner Depos 36:109–124
Weston R (2000) An overview of the structure, metamorphism, petrology, paragenesis and geochemistry of the Houdini Prospect, Cloncurry District, Mount Isa Inlier, NW Queensland. BSc (Honours) thesis, James Cook University, Townsville
Williams PJ (1998) Metalliferous economic geology of the Mt Isa Eastern Succession, Queensland. Aust J Earth Sci 45:329–341
Williams PJ, Skirrow RG (2000) Overview of iron oxide–copper–gold deposits in the Curnamona Province and Cloncurry District (eastern Mount Isa Block), Australia. In: Porter TM (ed) Hydrothermal iron-oxide copper–gold & related deposits: a global perspective. Australian Minerals Foundation, Adelaide, pp 105–122
Williams PJ, Dong G, Ryan CG et al (2001) Geochemistry of hypersaline fluid inclusions from the Starra (Fe oxide)–Au–Cu deposit, Cloncurry District, Queensland. Econ Geol 96:875–883
Xu G (2000) Methane-rich fluid inclusions in the Proterozoic Zn–Pb–Agdeposit at Dugald River, NW Queensland; potential as an exploration guide. Appl Geochem 15:1–12
Zheng Y-F (1999) Oxygen isotope fractionation in carbonate and sulfate minerals. Geochem J 33:109–126